2018

Effects of surface cross-linker on the binding properties of imprinted micelles

Shize Zhang
Iowa State University

Effects of surface cross-linker on the binding properties of imprinted micelles

by

Shize Zhang

A thesis submitted to the graduate faculty

in partial fulfillment of the requirements for the degree of

MASTER OF SCIENCE

Major: Organic Chemistry

Program of Study Committee:
Yan Zhao, Major Professor
Julia Zaikina
Brett VanVeller

The student author, whose presentation of the scholarship herein was approved by the program of study committee, is solely responsible for the content of this thesis. The Graduate College will ensure this thesis is globally accessible and will not permit alterations after a degree is conferred.

Iowa State University

Ames, Iowa

2018

TABLE OF CONTENTS

Page

LIST OF SCHEMES

LIST OF FIGURES

LIST OF TABLES

LIST OF CHARTS

Page

NOMENCLATURE

MIP	Molecularly Imprinted Polymer
FM	Functional Monomer
MINP	Molecularly Imprinted Nanoparticle
DCM	Dichloromethane
THF	Tetrahydrofuran

ACKNOWLEDGMENTS

I would first like to express the deepest appreciation to my research advisor, Dr. Yan Zhao, for his excellent guidance, persistent help, patience, and wisdom throughout my research work. Without him, this dissertation would not be possible.

I would also like to thank my program of study committee members, Dr. Julia Zaikina and Dr. Brett VanVeller for their insightful comments and encouragement. They all have dedicated their time to give me advice and useful ideas over the years.

My sincere thanks goes to the members of the chemical instrumentation facility including Dr. Sarah Cady, Dr. Shu Xu, Dr. Kamel Harrata, and Mr. Steve Veysey for their technical assistance to my research.

A special thanks to members of the Yan Zhao group for their valuable support and inspirational discussions.

Last but not the least, I would like to thank my father Mingquan Zhang and my mother Wenjuan Liu for supporting me spiritually throughout my study and my life in general.

ABSTRACT

Molecularly imprinted nanoparticles (MINPs), which have guest-complementary binding sites, are obtained by doubly cross-linking micelles containing appropriate guests. One of the most important building blocks of MINPs is the cross-linker that can profoundly affect the structure and property of MINPs. In the traditional method, 1,4-diazidobutane-2,3-diol is used as the cross-linker for the cross-linkable surfactants. In this work, a new cross-linker (Compound **11**) is used instead. This new cross-linker can improve the binding affinity between MINPs and their guests, due to the more rigid structure compared to that from 1,4-diazidobutane-2,3-diol. In addition, with a hydroxylamine functional group in the structure, the cross-linker allows MINPs to be post-modified to increase the path of the binding pocket, further improve the binding affinity.

CHAPTER 1.   GENERAL INTRODUCTION

Molecular recognition describes the phenomena of selective binding of molecule (i.e., guest) by a molecular host to form a supramolecular species through noncovalent interactions. [1,2] Molecular recognition is involved in practically all biological processes and, not surprisingly, attracts much attention in modern chemistry research. [2] In order to obtain high selectivity in the recognition, a binding cavity is required to have the shape, size, and functional groups complementary to the guest. Over the last deacde, a lot of different molecules and materials have been developed for molecular recognition, such as crown ethers, [3] cyclodextrin, [4] cucurbiturils, [5] and molecularly imprinted polymers [6].

Concept of Imprinting

The preparation of molecularly imprinted polymers (MIPs) is a process (Scheme 1.1) in which functional monomers (FMs) and cross-linkers are co-polymerized in the presence of guest molecules, which are referred to as template molecules. Before polymerization, the FMs form a complex with the guest molecules. After polymerization, the functional groups are held in position by the high cross-linking density of MIPs. Removal of template molecules will afford guest-complementary binding sites, which can rebind the template molecules. [7] In that way, the molecular information of the guest, including its size and shape, can be imprinted into the polymers. For good imprinting, the interactions between the template molecules and the FMs should be strong enough to form stable complexes during polymerization but not too strong to interfere with the removal of the template. [8] Three different types of interaction are frequently used to prepare molecularly imprinted polymers, covalent, noncovalent, and metal-ligand interaction. [9,10,11]
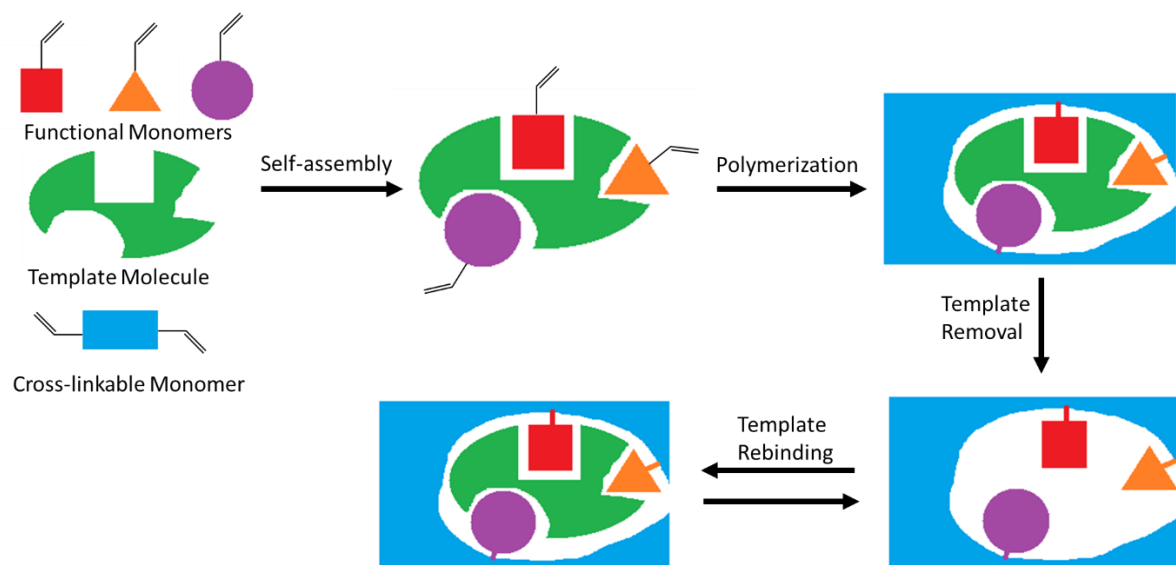
Figure 1.1 Schematic representation of molecular imprinting process

Imprinting by Covalent Interaction

Covalent imprinting uses functional monomers which form covalent bonds with the template. After polymerization, the covalent bonds between the polymer matrix and the templates are cleaved to remove the templates. As an example, a boronic acid is used for the covalent imprinting of compounds containing diols. Boronic acids form relatively stable trigonal boronate esters with 1,2 or 1,3-diols under relatively acidic or neutral conditions. Under more basic conditions, tetragonal boronate esters are formed. 4-Vinylphenylboronic acid, which is commercially available, is often used as the functional monomer for covalently imprinting diol compounds.[12] Besides, polymers imprinted by sugar (glucose, mannose, fructose, galactose) bound by two boronic acid groups can have very high resolution of racemates of sugars.[13,14] However, under some circumstances, three or more boronic acid groups bound to template molecules could result in poor selectivity. The main reason for this poor resolving might be the low rate of formation of polymer-guest complexes.[15]

Carboxylic acids can be imprinted covalently through ester formation.[16] After cleavage of ester bonds under suitable conditions, the rebinding can be achieved by reaction of hydroxyl groups with carboxyl chlorides, but the ester bonds are not good to be used for imprinting polymers due to slow binding kinetics and difficult removal of templates. A strategy proposed by Whitcombe to solve this problem is to use 4-vinylphenyl carbonate esters.[58] After polymerization, the carbonate bonds are cleaved efficiently with loss of CO_2. The hydroxyl groups left behind can bind alcohol via hydrogen bonding.

Schiff base is very suitable for imprinting aldehyde[18] or amine[19] template molecules due to the complete reversibility. But the low reaction rates make the rebinding process sluggish, limiting its application in chromatography.

Overall, the advantage of covalent imprinting is that the binding is strong and the functional groups of polymers are only associated with template binding sites. The disadvantage is that only a limited number of guest compounds can be imprinted by this approach and the binding is very difficult to reach equilibrium.

Imprinting by Noncovalent Interaction

Noncovalent imprinting uses functional monomers which interact with template molecules by noncovalent interactions. The interactions between the functional monomers and the template molecules during the polymerization are the same as those between MIPs and the guest molecules in the rebinding.[20] Hydrogen bond, electrostatic, and hydrophobic interactions are noncovalent interactions commonly used for imprinting. Because functional monomers and template molecules are in rapid equilibrium in solution, in order to ensure that the template molecules are bound to the functional monomers during polymerization, the ratio of functional monomers and template molecules are often quite high, sometimes over 4 : 1.[8] Many functional monomers for noncovalent imprinting have been developed. For

instance, methacrylic acid has been used for the imprinting of templates such as hydroquinidine,[21] steroids[22] and cyclic peptides.[23] 4-Vinylpyridine has been used for imprinting guest molecules such as bisphenol A.[24]

Electrostatic interactions might be the most widely used non-covalent interactions for imprinting. Many amine[25], acid[26], and phosphate[27] compounds have been imprinted by using electrostatic interactions. Although this type of interaction is strong, it alone can not bring good selectivity to the imprinted polymers.[28] To solve this problem, another interaction is often employed. For example, introduction of hydrogen bonds is very helpful to improve the selectivity. Not surprisingly, if hydrogen bond is the only interaction during the polymerization and rebinding process, the selectivity is also bad.[8] Covalent interaction can also be used in combination with non-covalent interaction to obtain higher selectivity.[29]

Noncovalent imprinting has several advantages over covalent imprinting, such as less restriction for guest compounds, faster rebinding, and more complete removal of templates after polymerization. However, there are still some notable drawbacks with this method. The biggest issue of noncovalent imprinting may be nonspecific binding. Because functional monomers and template molecules are in rapid equilibrium during the polymerization, there are always some dissociated functional monomers in the solution which create nonspecific or low-affinity binding sites after polymerization. Thus, functional monomers which have a strong stoichiometric binding (for example, a 1 : 1 ratio) with guest molecules have been designed.[30] In this case, the interaction between functional monomers and templates is strong enough (the association constant is larger than 10^3 M^{-1}) to push the equilibrium to the side of complex. Through the usage of stoichiometric noncovalent FMs, the amount of nonspecific binding sites can be reduced dramatically.

Imprinting by Metal Complexation

Metal complexation imprinting was first reported by Yuki Fuji.[31] By using this method, he and his co-workers imprinted N-benzyl-D-valine as the template molecule successfully. They used a chiral Schiff base ligand as the functional monomer, to form a Co^{2+} complex **1** with N-benzyl-D-valine and a high chiral selectivity (the enantiomeric excess > 95.5 %) was obtained. The chiral selectivity is believed to come from the cavity effect.[31] Then many different compounds, such as amino acids, [32] peptides,[33] and proteins[34], have been imprinted via different metal complexes.

Metal complexation is very promising for imprinting. Besides, the strength of the complexation can be controlled by experimental conditions.[8] Another advantage of this method is that there is no excess of dissociated functional monomers during the polymerization which lead to nonspecific binding sites. However, the kinetics of this kind of binding usually is too slow for applications in chromatographic separation.[8]
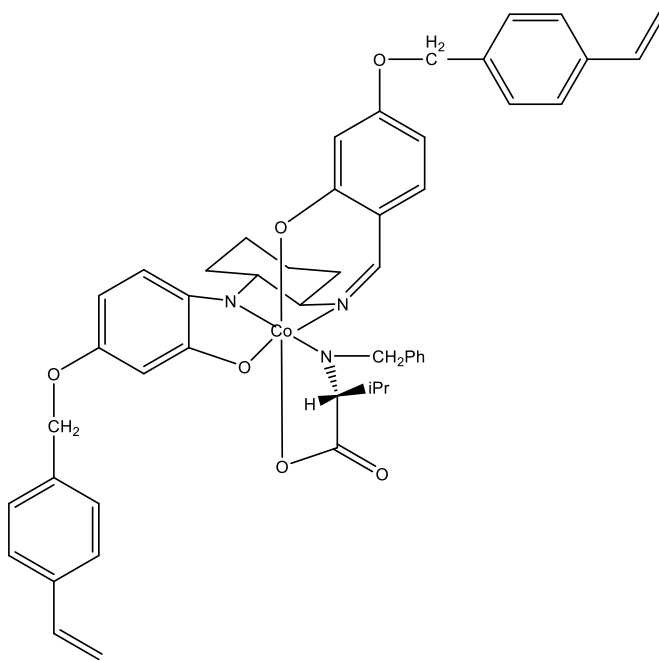
Figure 1.2 Co^{2+} complex **1** for imprinting

Structure of Molecularly Imprinted Polymers

Most molecularly imprinted polymers have macroporous structures because the pores can lead to a good accessibility for the binding sites by the guest molecules. Those macroporous structures are obtained by using a large amount of cross-linking agents (up to 90%)[8] in the presence of a porogen. After polymerization, the porogen is removed, which leaves pores in the polymer permanently. These large pores, with a diameter around 10-60 nm, give the synthetic polymers a relatively large inner area (around 50-600 m^2/g) and make most of the imprinted microcavities (diameter around 0.5-1.5 nm) accessible. Because of the property of cross-linked polymers, the size of these pores will change during swelling, but usually will not change much.[35]

The conditions for polymerization have been studied and optimized by Wulff.[36] In order to obtain molecularly imprinted polymers with good mechanical and thermal stability, the ratio of monomers and porogens should be around 1:1 (ml : g). Although different type and quantity of porogens being used during the polymerization will affect the morphology of polymers significantly, its effect on selectivity of molecularly imprinted polymers is very small.[37]

The key factor which has a strong influence on the binding selectivity is the type and quantity of the cross-linking agent.[38] For example, Wulff used different amounts of three cross-linking agents (ethylene dimethacrylate, divinyl benzene, and tetramethylene dimethacrylate) to prepare molecularly imprinted polymers with phenyl-D-mannopyranoside as the template molecule.[8] The results indicate that, when the concentration of cross-linking agents was lower than 10%, the synthetic polymers did not have any selectivity for racemic phenyl-D,L-mannopyranosides, no matter which cross-linking agents was used. If the cross-linking density of polymer matrix is not high enough, the shape of the cavities apparently can

not be maintained. When the amount of cross-linking agent was increased to 50%, same selectivity was obtained and the ee value was around 20%. Further increase of the cross-linker from 50% to 70% increased the ee value to 50%. 90% Cross-linking agent further increased the ee value to 57%. These results all indicate that cross-linking density plays a very important role in the rigidity of the binding sites, which affects the selectivity of molecularly imprinted polymers.

However, too high rigidity can be also problematic. Wulff also tried 95% cross-linking agent, but the selectivity of divinyl benzene was the smallest one in those three cross-linking agents. Because the structure of divinyl benzene is too rigid which increases the stiffness of structure dramatically, the accessibility of imprinted microcavities is decreased. Tetramethylene dimethacrylate was the mediocre one among the three cross-linking agents because the structure of tetramethylene dimethacrylate is too flexible, which can not give enough stabilization to the microcavities. Ethylene dimethacrylate was the best one because it ensures enough accessibility of microcavities and enough rigidity of polymer matrix. Overall, a compromise between high rigidity and enough flexibility for the microcavities is the best for most molecularly imprinted polymers. Thus, very rigid divinyl benzene and a more flexible styrene-based as cross-linking agent were used together to prepare synthetic polymers. This polymer, swelling in solvent which contains template molecules, functional monomers and ethylene dimethacrylates, is polymerized second time to obtain not only good selectivity, but also good thermal and mechanical stability.[8]

A lot of different cross-linking agents have been investigated in the same way.[39] Ethylene dimethacrylate is often a preferred choice because of its moderate rigidity and low cost. In addition, molecularly imprinted polymers prepared with a high level of ethylene

dimethacrylate has usually very good mechanical and thermal stability. Chromatographic columns, of which stationary phase is molecularly imprinted polymers, do not lose their selectivity even at 80 °C and 6-10 Mpa during a period of constant use over several months.[37] Synthetic polymers made with divinyl benzenes lose the selectivity at 70 °C.[36] Chiral cross-linking agents can not give better resolution of racemic compounds.[39] Andersson et al. prepared a cross-linker from L-phenylalanine for molecularly imprinted polymers.[59] The obtained synthetic polymers did not show selectivity over racemic guests.

The accessibility of imprinted microcavities have also been studied.[8] If the guest molecules are linked with functional monomers through non-covalent bonds, 90% of templates can be removed after polymerization. The remaining 10% guest molecules, which are embedded permanently in the polymer matrix, are normally "locked" inside the highly cross-linked part of the synthetic polymers and not accessible for reactions. About 80-90% of the empty microcavities can rebind guests when treated with an excess amount of template molecules. If the guest molecules are bound to functional monomers via covalent interactions, only 10-15% of guests can be removed after polymerization and around 90% of empty microcavities cannot be reoccupied by guest molecules, resulting in very low capacity. In addition to the type of imprinting, the porosity and inner surface area also affect the accessibility. One can use BET measurement and electron microscopy to characterize the porosity of molecularly imprinted polymers at dry state.[25] The porosity of synthetic polymers can be measured by using inverse gel permeation chromatography.[36] The results indicate that, although there are some small pores which would hinder the rebinding process, their population proportion is relatively small.

Applications of Molecularly Imprinted Polymers

Membranes and Sensors

Because of inherent selectivity for predetermined compounds and mechanical stability of molecularly imprinted polymers, many researchers explored their applications in sensing and membrane separation.

Fluorescence sensing is a very popular method of chemosensing. Due to the excellent sensity of fluorescent sensors, methods of incorporating fluorophores into imprinted polymers to obtain fluorescence sensors have been developed. The first reported design of this kind of sensors was published in 1996.[40] Piletsky et al. used sialic acids as template molecules, which were covalently bound to vinylphenylboronic acids. After polymerization and removal of templates, the polymers were treated with a fluorescent agent (phthalaldehyde) and 2-mercaptoethanol. An increase of fluorescence intensity during the rebinding process was observed. The detection limit of sialic acids reached to micromolar range in this method.

Another common way to introduce fluorophores is to use functional monomers which have a fluorescent moiety. During the rebinding process, the binding between functional monomers and guest molecules will lead to a change the electronic properties of the fluorophore, which would cause fluorescent signal's change. For example, Wang synthesized a fluorescent functional monomer **2** which has an anthracene moiety.[41] They used this functional monomer to imprint sugar templates via boronic acids. During the rebinding step, the signal intensity would change because of photoelectron transfer.
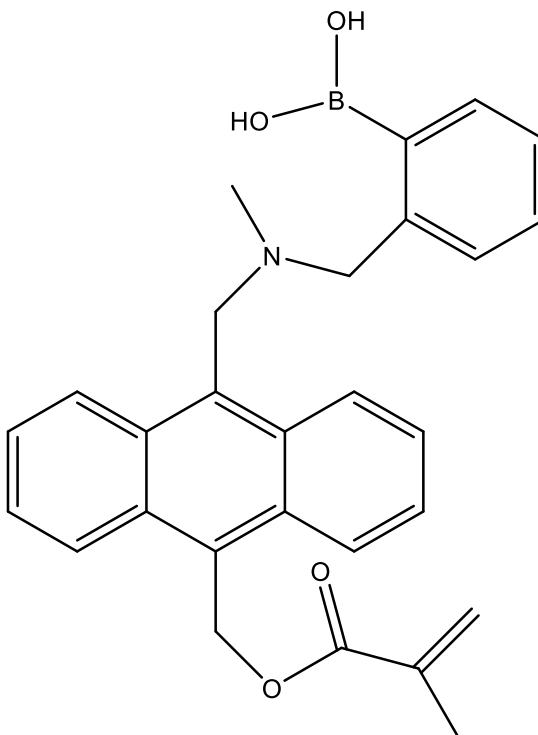
Figure 1.3 Functional monomer **2** synthesized by Wang

Although fluorescence-based molecularly imprinting polymer sensors have high sensitivity, optical molecularly imprinting polymer sensors have the advantage of simplicity. Levi et al. designed a practical optical HPLC device with molecularly imprinted polymers as the stationary phase for detection of antibiotic chloramphenicol.[42] This method is based on the displacement of chloramphenicol-methyl red dye **3** by chloramphenicol from polymers imprinted by chloramphenicol, which leads to a change in absorbance at around 460 nm. The response is linear when the concentration of chloramphenicol is between 3 and 1000 µg/ml.
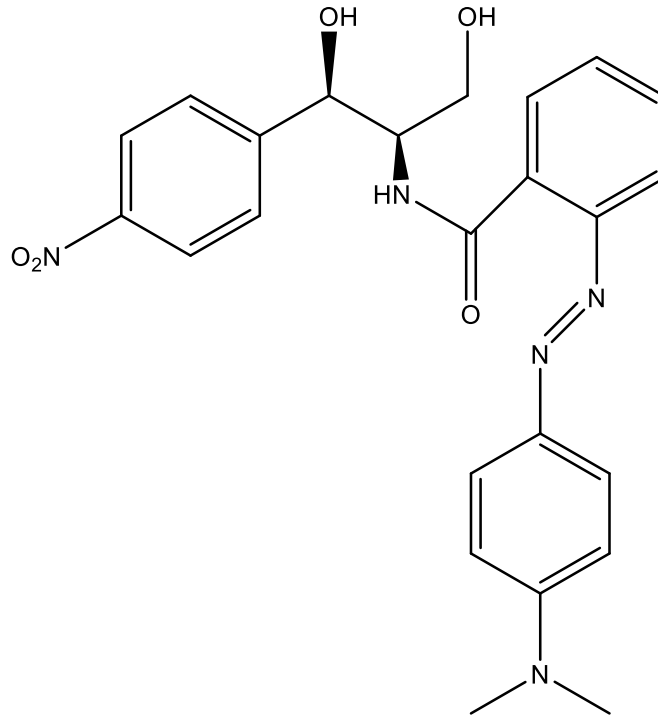
Figure 1.4 Chloramphenicol-methyl red dye **3** synthesized by Levi

Marx-Tibbon et al. reported a photostimulated molecularly imprinted polymers which exhibits a selective transport property for template molecules.[43] They prepared a poly(acrylamide-co-acrylic acid-coacryloylmerocyanine) molecularly imprinted polymer membrane with tryptophan as the template. Then the polymer membrane was put in the middle of two chambers. Upper chamber contained a solution of 0.01 M^3 different substrates while water flowed through the lower chamber. By collecting the fraction of eluent, which at equal time interval they measured, the transport rate of the substrates are observed. By using this method, the selective transport of tryptophan through the polymer membrane was observed. When the merocyanine was converted to spiropyran by visible light, the permeability towards tryptophan was turned off. Further study indicated that the transport change was due to the loss of imprinted cavity effect during this conversion.
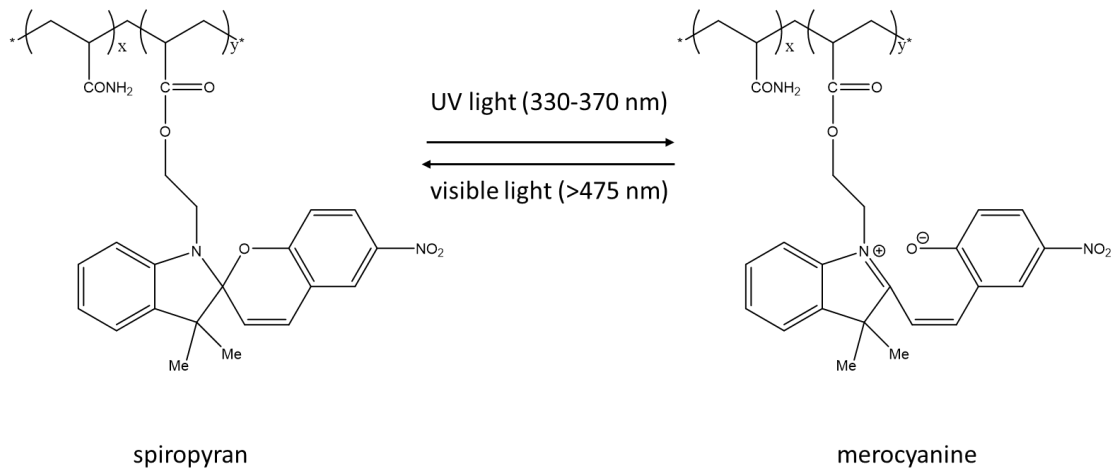
Scheme 1.1   Light induced converting process between spiropyran and merocyanine

Diffusion mechanism of molecularly imprinted polymer membrane for selective transport has been studied. Mathew-Krotz and co-workers prepared a polymer membrane by polymerization of methacrylic acid as the functional monomer in the presence of 9-ethyladenine as the template molecule.[43] Transport rate was measured by using an H-shaped chamber and the concentration of substrate of receiving cell was quantified by HPLC. They found that the transport rate of adenine was faster than that of other substrates, which was attributed to the imprinted binding sites. They proposed that the adenine was concentrated at the binding cavities, which increased the probability of diffusion through the membrane. This proposal was verified by the comparison with nonimprinting polymer membrane and the solvent effect on selectivity.

Chromatography

One of the most important applications of molecularly imprinted polymers is being used as the stationary phase for chromatography.

Wulff conducted a series of studies on the separation of racemic α-D-mannopyranoside and its derivative by polymers imprinted by α-D-mannopyranoside via boronic acids ester bonds.[29] In the beginning, the selectivity was good but the peak broadening made it impossible to separate racemic mixtures. After optimization of the eluent, temperature and modification of polymers, they achieved resolution of Rs=4.3 for racemic α-D-mannopyranosides. While most early works on separating saccharides used boronic acids for the imprinting, noncolvent MIPs have also been developed. Mayes et al. used polymers imprinted by p-nitrophenyl-α-D-galactoside or p-nitrophenyl-α-L-fucoside to obtain anomeric resolution for sugars.[45]

Molecularly imprinted polymers with peptides as template molecules have been used as the chiral chromatographic stationary phase. Ramstrom used dipeptide N-Ac-L-Phe-L-Trp- OMe as the template to prepare polymers with methacrylic acid as the functional monomer and ethylene glycol dimethacrylate as the cross-linker.[46] The cavities created by N-Ac-L-Phe-L-Trp- OMe had the racemic resolution up to 1.7. Larger peptides have also been used as templates to prepare polymers. For instance, Andersson et al. conducted the imprinting of Leu-enkephalin by using methacrylic acid as the functional monomer.[47] The polymers imprinted by Leu-enkephalin did not exhibit good recognition results because DMSO must be used as the solvent of polymerization due to the poor solubility of Leu-enkephalin in apolar solvent. Then they changed the template to Boc-LeuS-enkephalin and Leu-enkephalin anilide, which can be dissolved in apolar solvent. Both templates gave good recognition results.

Catalysis

Molecularly imprinted polymers may be used to mimic enzyme's functionality, with functional groups inside binding sites. Catalytic molecularly imprinted polymers normally

are prepared with an transition state analogue as the template, affording imprinted cavities in the shape of reaction intermediate. Because these cavities can stabilize the intermediate on the reaction pathway, the activation energy of the reaction can be lowered. The transition state analogue can not have the shape MIP-based exactly the same as the intermediate of lowest energy. However, MIP-based catalyst can be designed through this strategy.

Many MIP-based catalysts for hydrolysis reactions of amide and ester have been reported. For instance, Ohkubo designed a catalyst for ester hydrolysis of Z-L-Leu-PNP peptide.[48] By using a racemic transition state analogue of phenyl-1-benzyloxycarbonyl-3-methylpentylphosphonate as the template and functional monomers which contained L-histidine and quarternary trimethyl- ammonium groups (Scheme 1.3), stereoselective hydrolysis of Z-L-Leu-PNP peptide was achieved.
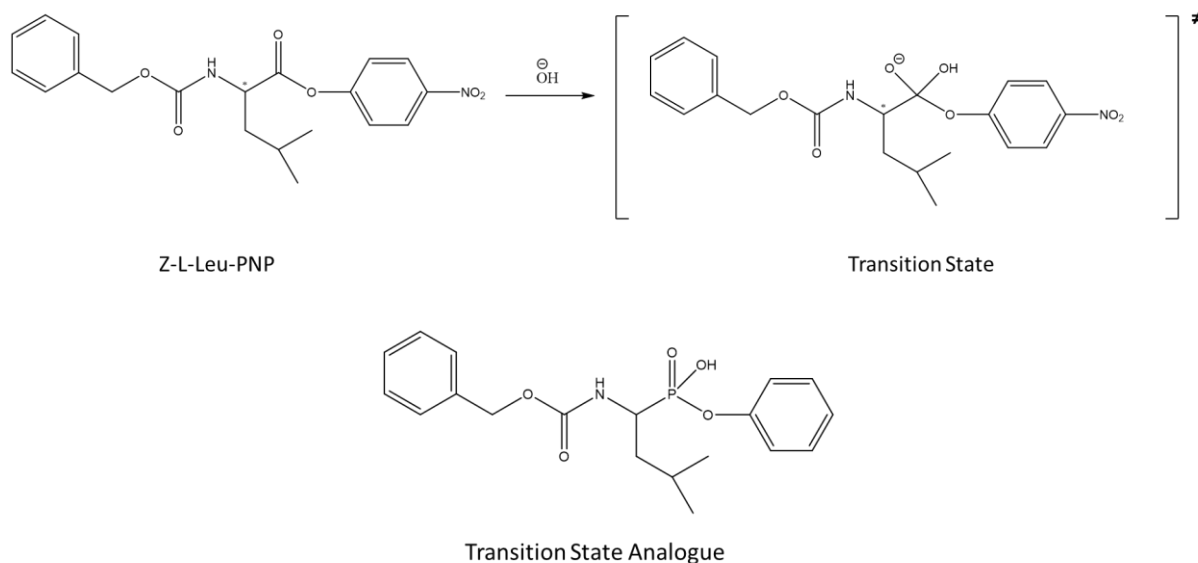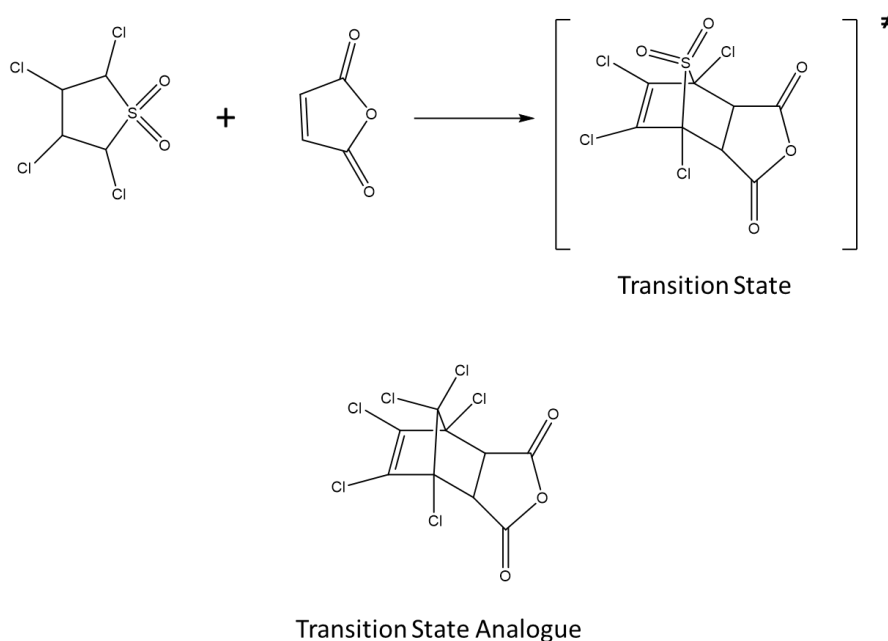

Scheme 1.2 Transition State Analogue for the hydrolysis of Z-L-Leu-PNP peptide

MIP-based catalysts for other types of reactions have also been developed. For example, Liu et al. used polymer imprinted by the transition state analogue to catalyze Diels-

Alder reaction (Scheme 1.4).[49] The reaction rate can be increased to 270 times compared to that of the uncatalyzed reaction.[49]

Transition State

Transition State Analogue

Scheme 1.3 Transition state analogue for the Diels-Alder reaction

Cell and Microorganism Recognition

Because molecularly imprinted polymers have potential applications in fundamental biology research, molecularly imprinted polymers for recognition of cell[50], bacteria[51] and virus[52] have been developed in the last decade. There are two strategies to design synthetic polymers for the recognition of cell and microorganism, cell-membrane-molecular imprinting and whole-cell-imprinting. Cell-membrane-molecular imprinting is to imprint exposed molecules on the surface of cells, such as polysaccharides and proteins. An alternative way is to imprint bioactive ligands which have specific strong interactions with certain cell membrane receptors.[53] Cell-membrane-molecular imprinting allows one to conduct indirect cell imprinting without using cells as templates. The method is very attractive due to the vulnerability of cells. Moreover, this method avoids the risk of infection when one tries to

imprint harmful bacteria and viruses. However, the most challenging step of this method is choosing proper cell membrane ligands as templates, on which the recognition performance depends. Compared to cell-membrane-molecular imprinting, whole-cell-imprinting does not need to worry about selecting cell membrane ligands because the entire cells are used as templates. Nevertheless, for mammalian cells, conditions of polymerization need to be mild and pre-treatment of cells is usually required because of the fluid mammalian cell membranes. Hence, whole-cell-imprinting is commonly used for imprinting bacteria and viruses due to their rigid shapes.

Like imprinting other small guests, introducing functional monomers with strong affinity towards cell membranes could lead to good recognition results. For example, Mohsen conducted electrochemical whole-cell-imprinting of bacterial cells by using 3-aminophenylboronic acids as functional monomers.[54] The boronic acid groups were bound to the cis-diols on the surface of bacterial cell membranes during the polymerization. After removal of template cells, good selectivity was obtained.

Another key factor to microorganism is the accessibility of imprinted cavities. Due to its large size compared to small molecules, imprinted cavities must be on the surface of polymer matrix.[55] To achieve that, several different methods have been employed by people, such as micro-contact stamping method, lithographic process, Pickering emulsion and colloidal imprints. Lithographic process and Pickering emulsion are quite similar, both benefit from that microorganisms tend to self-assemble on the water-oil interface. Lithographic process let the cell templates disperse and self-assembly on the surface of organic phase in aqueous media and then followed by polymerization. Pickering emulsion considers cells not only as templates but also particle stabilizers. The cells can self-assemble

on the water-oil interface and form a stable emulsion network with functional monomers. Micro-contact stamping method refers to that conduct conformal stamping of a template-immobilized layer on a polymer surface and then the imprinted cavities can be on the surface of polymer. Colloidal imprints is using inorganic shells to encapsulate cells and then followed by deposition of silica layer on the surface. After fragmentation, the colloid analogues are created for cell recognition.

# CHAPTER 2.   ENHANCED BINDING AFFINITY FROM STRUCTURE RIGIDITY EFFECT FOR MOLECULARLY IMPRINTED NANOPARTICLES

Introduction of Molecularly Imprinted Nanoparticles

In 2013, the Zhao group reported molecularly imprinted nanoparticles (MINPs) which can recognize bile salts.[55] A cationic surfactant with a methacrylate-terminated hydrophobic tail and a tripropargylammonium headgroup was used to form micelles in the presence of bile salts and divinyl benzene (DVB) in water. After surface cross-linking with a diazide via the click reaction, surface functionalization with an azido sugar derivative, and radical core-cross-linking under UV light, nanoparticles with imprinted pockets can be obtained (Scheme 2.1). Molecularly imprinted nanoparticles have sizes similar to proteins'(around 5 nm), good water solubility and guest-shaped hydrophobic pockets. The binding affinity between the guests and MINPs can be measured by fluorescence and ITC titration. In the same work, the effect of cross-linking density was investigated by changing the amount of divinyl benzene. When the amount of DVB was 0.5 equiv. to the surfactant, no selectivity towards the template molecule was found. When the amount was increased to 1 equiv, good selectivity was observed. Thus, similar to other MIPs, cross-linking density is very important to the molecular recognition of MINPs.
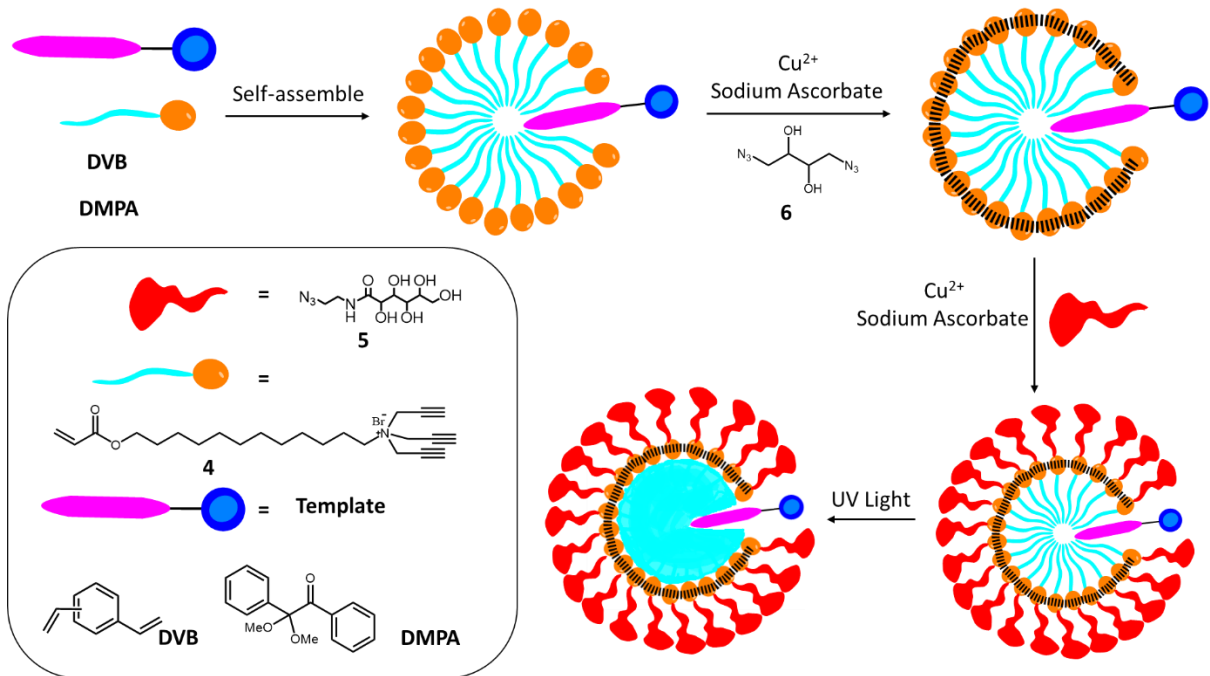
Scheme 2.1 Schematic representation of MINPs preparation

In addition to bile salts, MINPs can be used to recognize other biomolecules, such as sugars[56] and peptides[57] in the presence of functional monomers. Gunasekara et al. used a boroxole-containing styrenic monomer with the amount of 2 equiv. to the sugar template, to prepare MINPs.[56] The obtained MINPs presented great selectivity over monosaccharides and oligosaccharides in water. Fa et al. used functional monomer **7** containing a crown ether group to imprint basic peptides.[57] The data indicated that a 1:1 ratio between functional monomer **7** and the amino groups of the peptides was optimal.
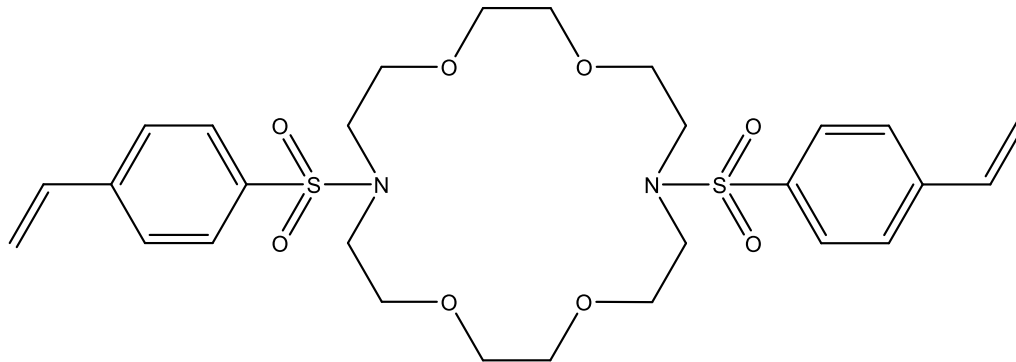
Functional monomer **7** used by Fa

New Design of Cross-linker

The surface cross-linker used in previous studies was cross-linker **6**, which has a

flexible carbon backbone. Two hydroxyl groups on the backbone gave cross-liner **6** sufficient

water-solubility. In order to understand how the rigidity of surface cross-linker affects the

binding affinity of MINPs, Arifuzzaman et al. designed a surface cross-linker **8** containing a

more flexible carbon backbone compared to cross-linker **6** and a sugar tail to interact with the

hydrophilic moiety of the guest molecules.
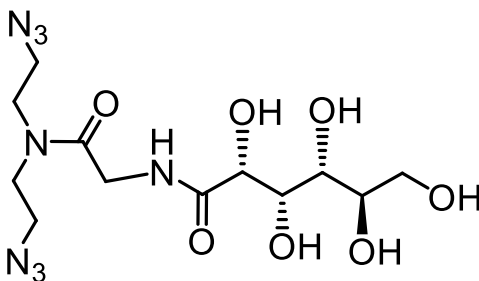
Cross-linker **8** designed by Arifuzzaman

The binding study indicates that the structure of cross-linker **8** is too flexible for

imprinted pockets to maintain their shape. However, the sugar tail can introduce extra

hydrogen-bonding interactions on the surface of MINPs with guests containing multiple hydroxyl groups.

These results suggest shortening the distance between the two azides in the surface-cross-linker could be beneficial. The first new design is cross-linker **10** with three carbons between the two azides. Cross-linker **10** can be easily synthesized by reduction of compound **9** (Scheme 2.2). However, the compound was not soluble in water with only one hydroxyl in the structure.
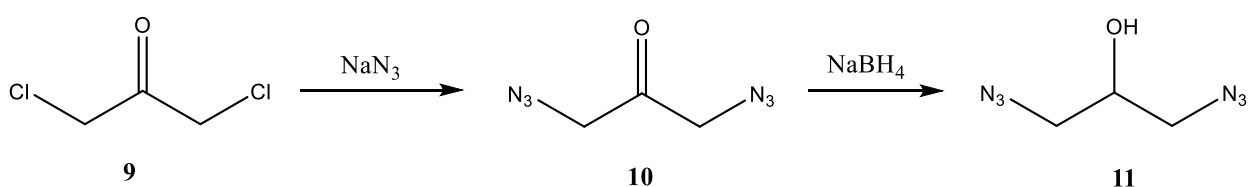
Scheme 2.2 Preparation of cross-linker **11**

To further increase the water solubility of cross-linker **11**, several attempts were made. Scheme 2.3 shows the synthesis of three-carbon-tethered diazide with three hydroxyls. However, the second step to obtain compound **13** failed because transformation of the carbonyl group to the hydroxyl group decreased the electrophilicity of the carbon linked with chloride, which made the azide substitution unable to happen.
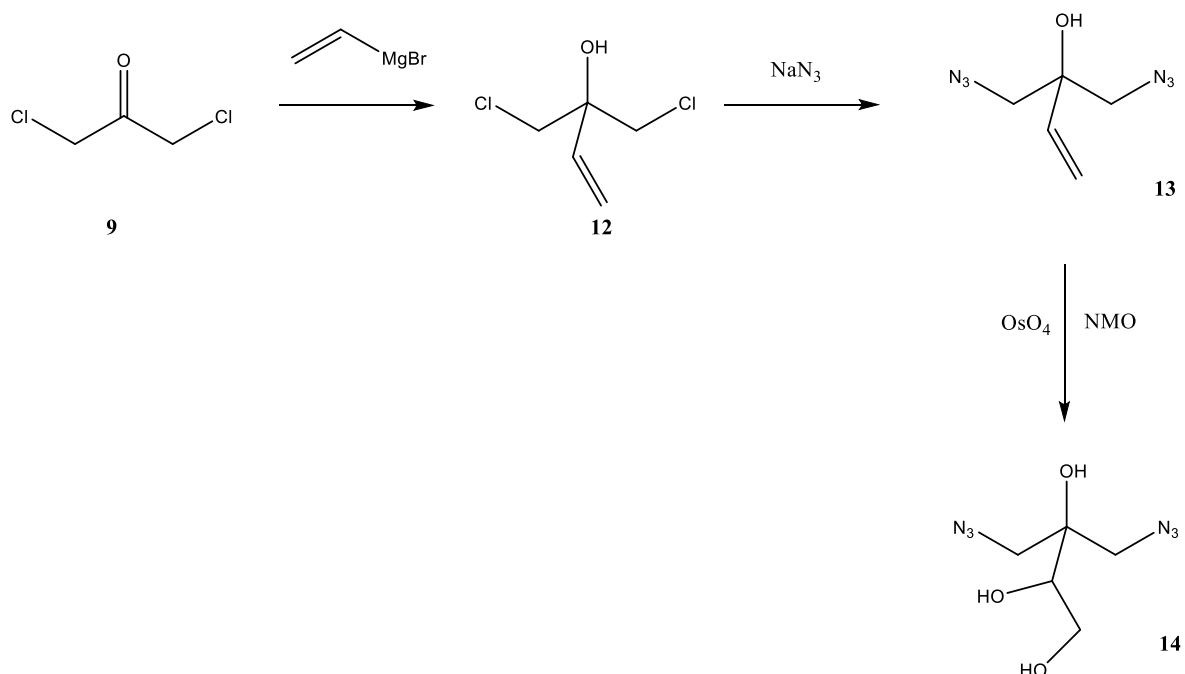
Scheme 2.3 Introducing more hydroxyl groups by Grignard Reaction

Mannich reaction can be used to alkyl the α position next to a carbonyl functional group, by a primary or secondary amine and formaldehyde. Thus, it represents another way to introduce hydrophilic groups on the α position of compound 3 (Scheme 2.3).
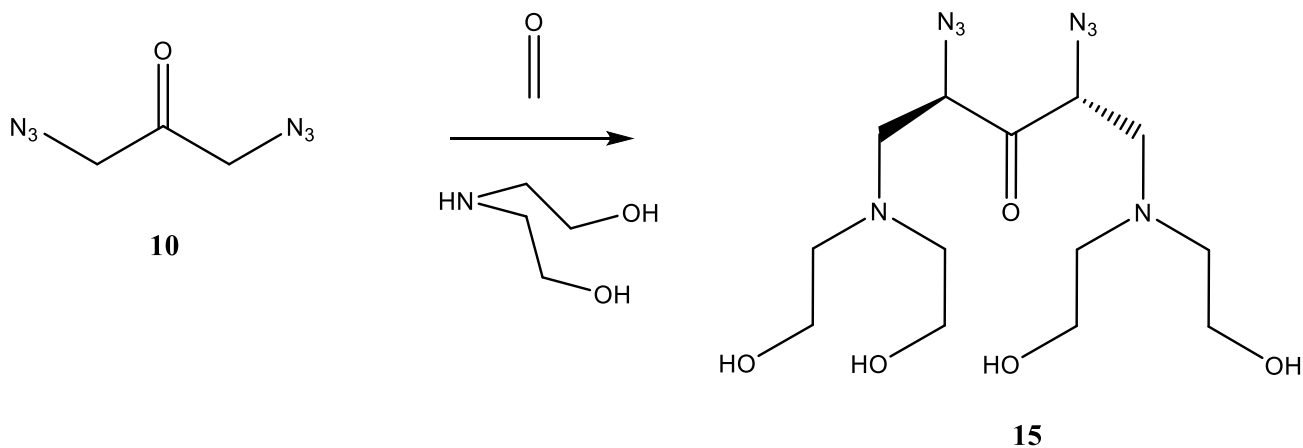
Scheme 2.4 Introducing more hydroxyl groups by Mannich Reaction
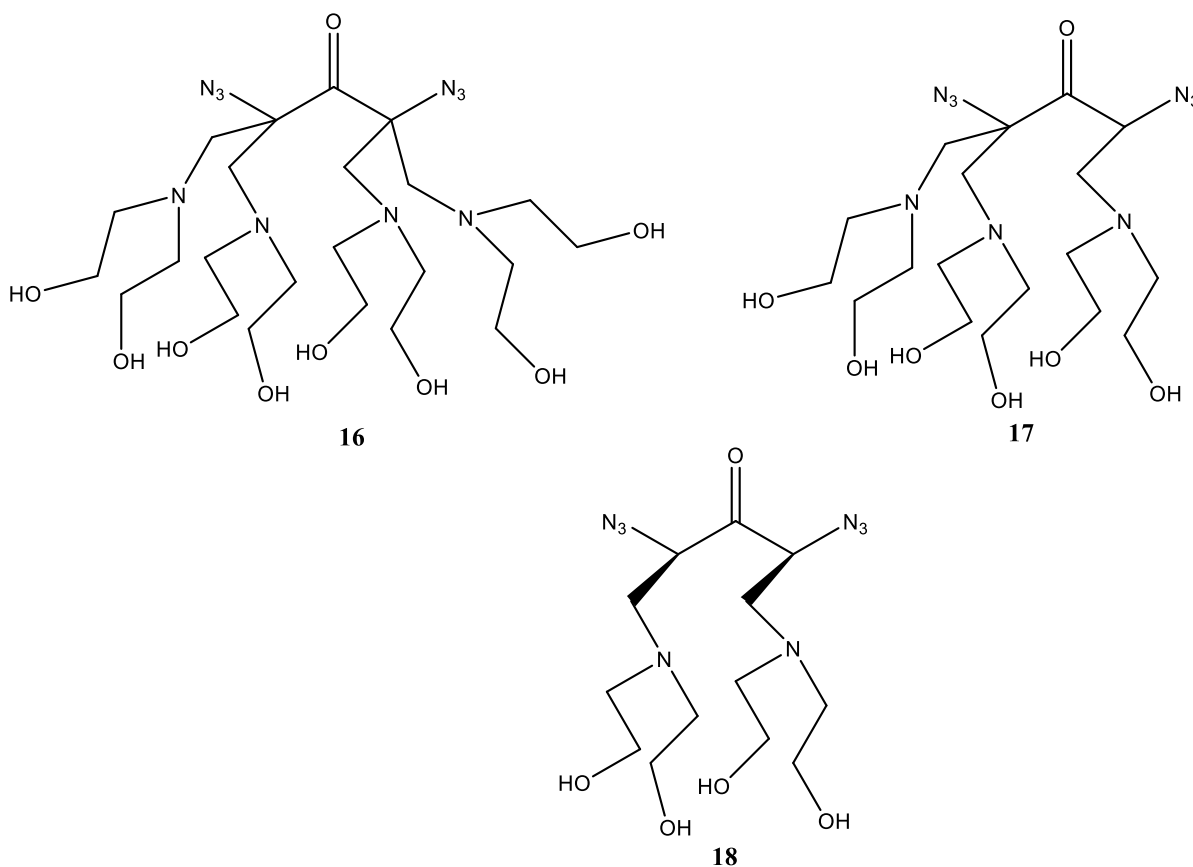
Although some product was identified by mass spectrometry, many side products also formed, leading to a very low yield. It was also difficult to control the stoichiometry of the reaction, meaning many other highly polar products could form as well.

Chemical structures of all possible side products

Hydroxylamine can form oxime with the carbonyl group of ketones or aldehydes. Oximes tend to have good stability in water. Due to its facile formation mild conditions, oxime is widely used in biomolecular modification.[60] The third design, thus, was to use oxime to link a sugar ligand with compound **10** (Scheme 2.4). The sugar group potentially can provide not only good water solubility but also extra hydrogen bonds with guests containing polar moieties.
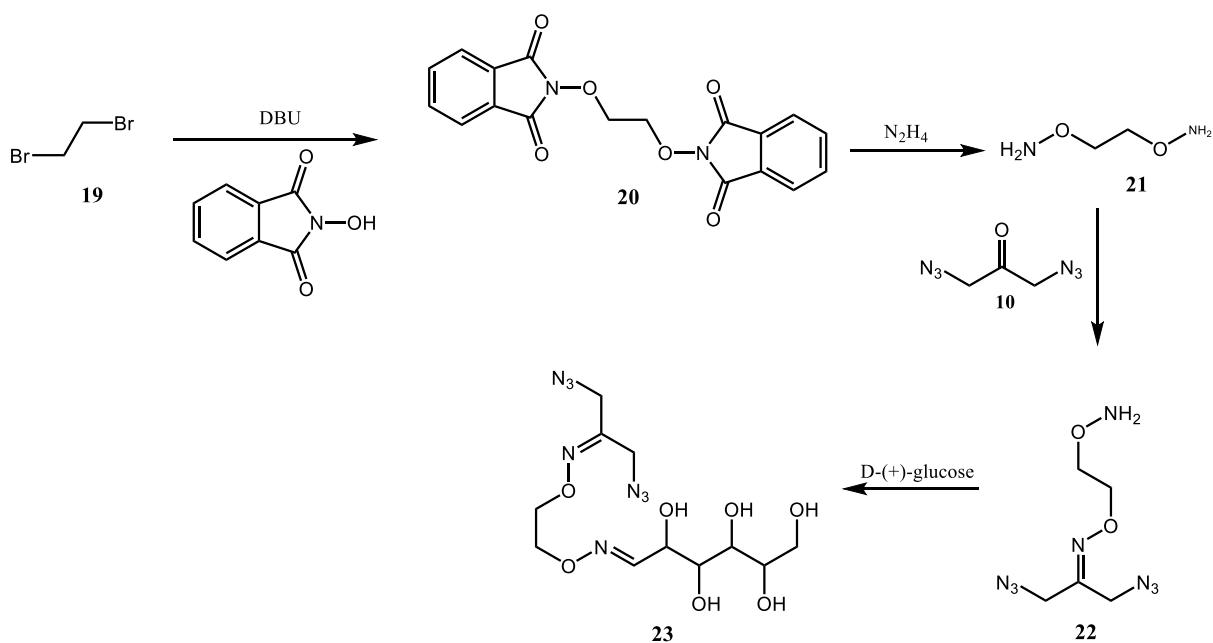
Scheme 2.5 Synthesis route of cross-linker **23**

The overall yield of cross-linker **23** (E/Z=4:1) was 22%. Although the overall yield was modest, only the third step in this four-step synthesis required purification by column chromatography. With the hydroxylamine group on compound **22**, post-modification of MINPs is also possible, enabling more possibilities to study how the surface structure affects the property of MINPs.

Binding Study of New Cross-linkers

In order to understand the surface cross-linker's effect on MINPs, three different templates were chosen. Compound **24** and compound **25** were used to evaluate the selectivity of MINPs. Compound **826** was used to see how the sugar tail on the cross-linker **23** interact with templates. Cross-linker **6**, **11** and **23** discussed before were used.
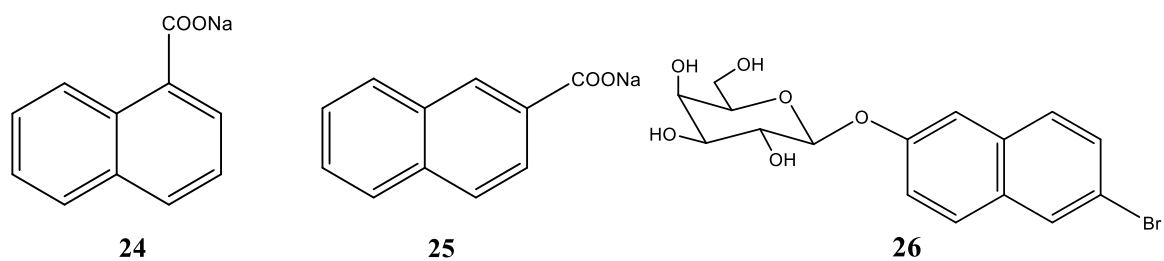
Structures of templates used in study
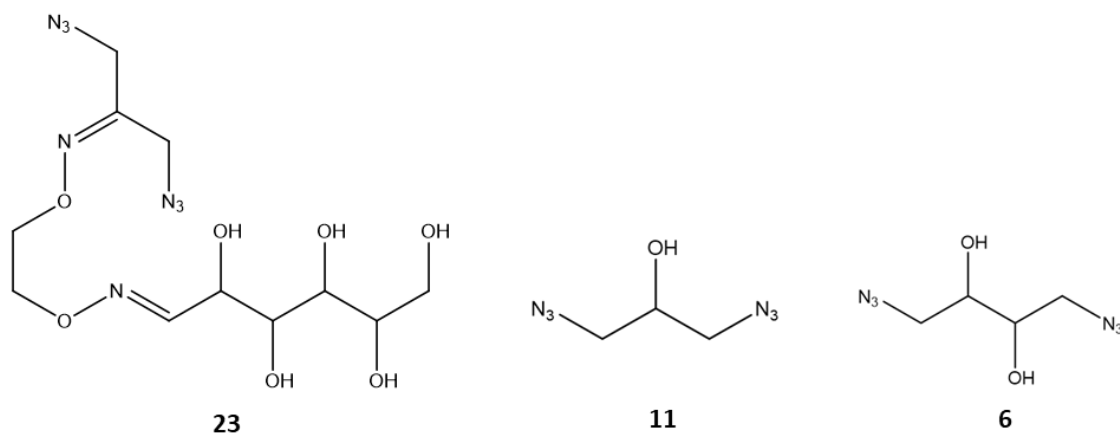
Structures of cross-linkers used in study

All the MINPs were prepared via the standard MINP preparation procedure (Scheme 2.5). Because all three templates are fluorescent, the removal of templates can be monitored by fluorescence (Figure 2.1). After each washing, the fluorescence intensity of the eluent was measured. It turned out that after four times of washing, the eluent's fluorescence intensity became very low, regardless of the cross-linker used. However, the fluorescence of template **24** and **26** was too weak in the buffer to conduct fluorescence titration to measure the MINP's binding property. Thus, all the binding constants were measured by ITC titration in 50 mM Tris buffer at 25 °C.
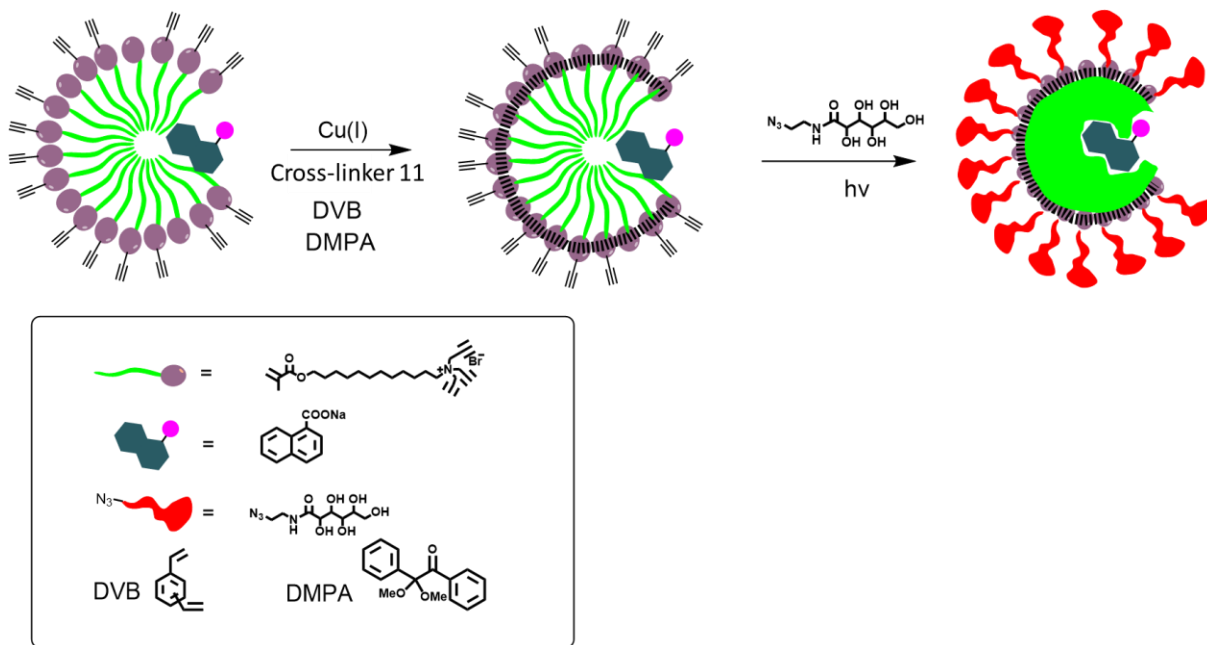
Scheme 2.6 Schematic representation of MINPs preparation

Figure 2.1 Guests' removal monitored by fluorescence

Table 2.1 Binding data for MINPs

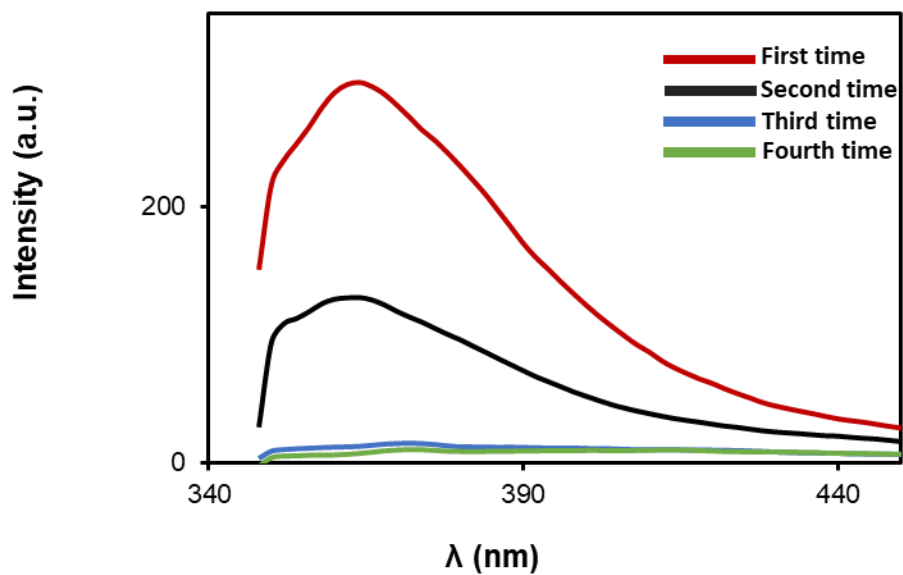| Entry	MINPs	Guest	K_a ($\times 10^5$ M^{-1})	N	ΔG (kcal/mol)	ΔH (kcal/mol)	TΔS (kcal/mol)
1	MINP$_{1.2equiv\mathbf{23+5}}$ (**24**)	**24**	20.7±3.0	0.86±0.08	-8.7	-107.6±11.7	-98.9
2	MINP$_{1.2equiv\mathbf{11+5}}$ (**24**)	**24**	2.28±0.71	1.07±0.35	-7.3	-20.8±8.2	-13.5
3	MINP$_{1.2equiv\mathbf{6+5}}$ (**24**)	**24**	6.46±2.05	0.71±0.08	-7.9	-11.04±1.8	-3.5
4	MINP$_{1.2equiv\mathbf{23+5}}$ (**24**)	**25**	4.04±1.15	1.12±0.05	-7.6	-5.3±0.4	2.3
5	MINP$_{1.2equiv\mathbf{6+5}}$ (**24**)	**25**	1.25±0.14	0.74±0.08	-7.0	-14.9±2.0	-7.9
6	MINP$_{1.2equiv\mathbf{23+5}}$ (**25**)	**25**	30.8±3.0	1.08±0.01	-8.8	-103.3±1.8	-94.5
7	MINP$_{1.2equiv\mathbf{6+5}}$ (**25**)	**25**	7.59±0.56	1.02±0.01	-8.1	-20.6±0.2	-12.5
8	MINP$_{1.2equiv\mathbf{23+5}}$ (**25**)	**24**	4.25±1.45	0.89±0.12	-7.7	-2.1±0.4	5.6
9	MINP$_{1.2equiv\mathbf{6+5}}$ (**25**)	**24**	1.20±0.08	1.15±0.03	-7.0	-3.8±0.1	3.2
10	MINP$_{1.2equiv\mathbf{23+5}}$ (**26**)	**26**	11.2±3.3	1.07±0.06	-8.3	-22.7±1.8	-14.4
11	MINP$_{1.2equiv\mathbf{6+5}}$ (**26**)	**26**	2.84±0.72	0.84±0.14	-7.5	-41.8±8.5	-34.3

[a] The titrations were generally performed in duplicates in 50 mM Tris Buffer (PH=7.3) and the errors between the runs were <20%. [b] The subscript denotes the surface-ligand (**Compound 5**) and cross-linker (**6, 11** and **23**) used in the MINP synthesis and the number in parentheses (**24**–**26**) denotes the template molecule.

MINP(**24**) displayed significant selectivity for the template in comparison to its isomer, regardless of the surface-cross-linker used. With **6** used in the preparation, it showed a smaller binding constant for guest **25**, with $K_a = 1.25 \times 10^5$ M^{-1} (entry 5). MINP(**24**) prepared with C3 diazide **23** also displayed a weaker binding for **25**, with $K_a = 4.04 \times 10^5$ M^{-1} (entry 4). As far as the difference in binding free energy between the template (**24**) and its isomer (**25**) is concerned, MINP prepared with **6** gave 0.8 kcal/mol and MINP prepared with **23** afforded 1.1 kcal/mol. The ratio between the binding constants for the matched/mismatched guests was 5.2 with **6** and 5.1 with **23**. Thus, the binding selectivity stayed nearly constant regardless of the surface-cross-linker.

MINP(**25**) showed a similar trend in the binding affinity. For example, the replacement of the C4 cross-linker (**6**) with the C3 cross-linker (**23**) increased the K_a value for the template from 7.59 to 30.8× 10^5 M^{-1}, by ~4-fold (entries 10 and 11). The binding selectivity basically

stayed the same. The difference in binding free energy between the template (**25**) and its isomer (**24**) was 1.1 kcal/mol with either surface-cross-linker.

What could be the possible reason for the improved binding affinity but similar binding selectivity? An important clue could be the fact that the shorter surface-cross-linker (**23**) strengthened the binding for both the matched and mismatched guest molecules. In other words, the higher surface-cross-linking density from **23** did not improve the complementarity between the template and the imprinted binding site significantly, or the change would help the template more than its structural analogue. A possible explanation for the results is that the shorter cross-linker did a better job in preventing the collapse of the binding pocket in the aqueous solution than the longer, more flexible one. Prior to the binding, the strong cohesive energy of water and the unfavorable exposure of the vacated hydrophobic imprinted site to water create a very unfavorable situation. Although this unfavorable situation is the exact driving force for the rebinding of the template afterwards, the system could also mitigate the situation by a partial or complete collapse of the binding site. On the other hand, because MINP was prepared through surface-core cross-linking of the micelles with the template trapped inside, the cross-linked network favors the binding site being open, in the non-collapsed state. Since the shorter cross-linker helped both the matched and mismatched guests, we suspect that the surface-cross-linking plays an important role in preventing the collapse of the binding pocket. Regardless of the exact reason for the nearly constant binding selectivity, a shift of the carboxylate in one position (from **24** to **25** or vice versa) could be detected easily by our MINPs with either cross-linker, highlighting the success of the molecular imprinting.

Another interesting trend observed in our binding data is that the mismatched guest—i.e., **25** for MINP(**24**) and **24** for MINP(**25**)—gave quite similar binding constants, about 1.20–1.25

$\times 10^5$ M^{-1} with **6** as the cross-linker and 4.0–4.3 $\times 10^5$ M^{-1} with **23**. Most likely, these numbers simply reflect the general driving force for these isomeric guest molecules to enter a hydrophobic binding sites. In contrast, a larger difference was observed in the binding constants for the MINPs and their own templates: 20.7 $\times 10^5$ M^{-1} for **24** by MINP(**24**) and 30.8 $\times 10^5$ M^{-1} for **25** by MINP(**25**) (Table 1, entries 1 and 6). Not only so, the binding between **25** and its own MINP was always stronger than that between **24** and its own, regardless of the surface-cross-linker. This is a very interesting trend because the two compounds are isomers and have identical hydrophobes and the same hydrophilic carboxylate. The only difference between the two is the location of the carboxylate.

The carboxylate of template **24** and **25** is ionic and highly hydrophilic. It is expected to stay on the surface of the micelle during imprinting and binding, most likely ion-paired with one of the cationic surfactant headgroups. Such an arrangement also ensures the solvation of the carboxylate by water molecules, which tends to be very strong for ionic groups. Because of this "hydrophilic anchoring", we expect the imprinted binding site for **25** to be deeper into the hydrophobic core of the cross-linked micelle than that for **24**.

Once the above picture is made clear, it seems fairly reasonable that the mismatched guest has the same driving force to enter the binding pocket, determined by the size of the pocket and the exposed hydrophobic surface area of the guest, with the latter being constant for the two isomers having the same naphthyl hydrophobe. The difference between the two surface-cross-linkers themselves for the mismatched guests (i.e., 1.20–1.25 $\times 10^5$ M^{-1} with **2** and 4.0–4.3 $\times 10^5$ M^{-1} with **5**) was totally reasonable from viewpoint of collapsed versus non-collapsed binding sites: with the binding site kept more open by the shorter cross-linker, the overall driving force for any hydrophobic guest to enter the pocket should be higher.

What is the reason for the overall stronger binding for **25** and its own MINP? We suspect it is due to the polarity of the binding site itself. Generally speaking, the deeper the binding pocket reaches into the micellar core, the smaller is its polarity. Near the surface, MINP mostly consists quaternary ammonium groups, triazoles from the click reaction, and any carbons and other functional groups from the cross-linkers. For a shallow pocket created from **24**, the binding site near the surface is quite polar from these functional groups. Deeper into the core, the MINP consists of the hydrophobic chain of **25** and DVB; the polarity thus decreases significantly. A less polar binding pocket should be more poorly solvated than a more polar one and should give a larger hydrophobic driving force for the binding of **25** by its own MINP.

Table 1 also shows that the shorter surface-cross-linker helped the nonionic template **26**. The binding constant going from the longer **6** to the shorter **23** increased the K_a value from 2.84×10^5 M^{-1} to 11.2×10^5 M^{-1}, by 3.7-fold in this case (entries 11 and 10). Thus the effect of the replacement was nearly constant in all three templates (i.e., a 3-4-fold increase in binding constant). This independency from the substrates does seem to be consistent with the notion that the change was mostly in the MINP itself, as suggested by our binding-site-collapse model. The binding between **26** and MINP(**26**) was somewhat weaker than those between **24** or **25** and their corresponding MINPs. The difference probably reflected the favorable electrostatic interactions between the anionic templates and their cationic MINPs. We have shown previously that electrostatic interactions did play a significant role in the MINP binding when the surfactant and the template carried opposite charges.

**Surface Imprinting of Molecularly Imprinted Nanoparticles**

Compound **22** being used as surface cross-linker provided probabilities of post-modification for MINPs. To further study how the surface cross-linking density affected

MINPs' recognition, dialdehyde **27** and **28** was employed to conduct imprinting on the

surface of MINPs in the presence of aniline. Compound **27** was synthesized by using

Shankar's method[61] and compound **28** was commercially available.
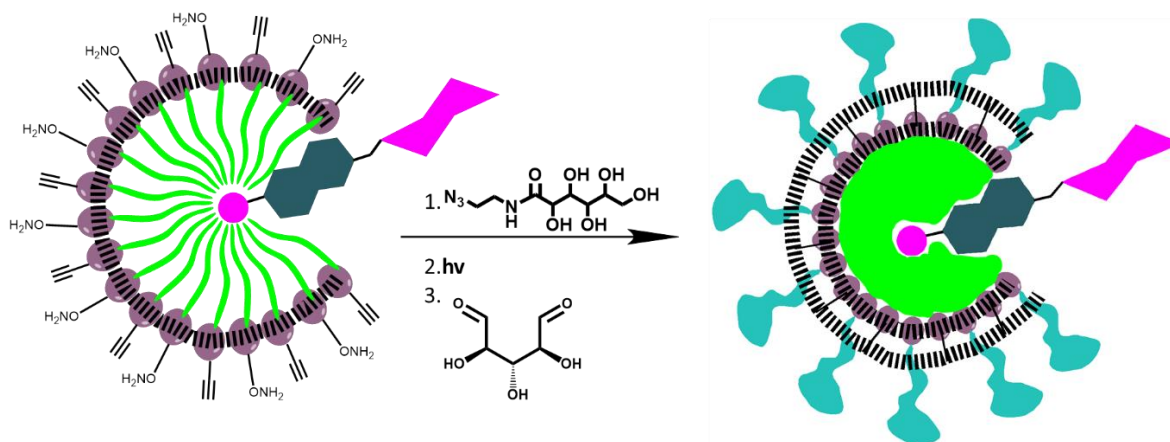
Scheme 2.7 Procedure for surface imprinting

27   **28**
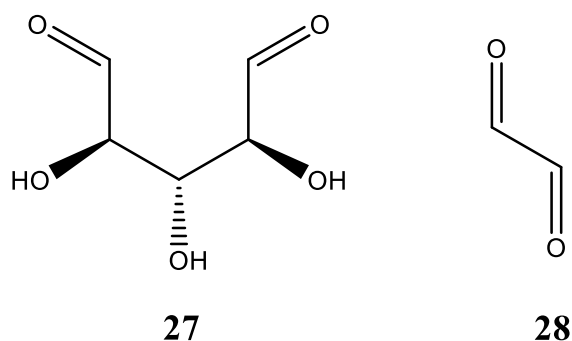
Chemical structures of dialdehyde **27** and **28**

Table 2.2 Binding data for surface-imprinted MINPs

Entry	MINPs	Guest	Ka $(\times 10^5$ M-1)	N	ΔG (kcal/mol)	ΔH (kcal/mol)	$T\Delta S$ (kcal/mol)
1	MINP$_{1.2equiv22}$ (**24**)	**24**	1.37 ± 0.63	1.03 ± 0.85	-7.0	-16.4 ± 15.2	-9.4
2	MINP$_{1.2equiv22+ 0.6equiv27}$(**24**)	**24**	12.5 ± 1.1	1.03 ± 0.01	-8.3	-75.6 ± 1.5	-67.3
3	MINP$_{1.2equiv22+ 0.6equiv27}$(**24**)	**25**	1.9 ± 0.5	1.01 ± 0.07	-7.2	-27.1 ± 2.6	-19.9
4	MINP$_{1.2equiv22}$ (**25**)	**25**	2.97 ± 0.18	1.02 ± 0.01	-7.3	-38.6 ± 0.4	-31.3
5	MINP$_{1.2equiv22+ 0.6equiv27}$(**25**)	**25**	33.7 ± 9.2	0.95 ± 0.03	-9.0	-15.0 ± 0.6	-6.0
6	MINP$_{1.2equiv22+ 0.6equiv27}$(**25**)	**24**	2.9 ± 2.1	0.91 ± 0.03	-7.5	-75.4 ± 3.2	-67.9
7	MINP$_{1.2equiv22}$(**26**)	**26**	2.31 ± 1.09	1.17 ± 0.07	-7.3	-35.0 ± 7.9	-0.09
8	MINP$_{1.2equiv22+ 0.6equiv27}$(**26**)	**26**	24.7 ± 3.8	0.88 ± 0.02	-8.6	-132.6 ± 2.8	-124.0

Table 2 compares the MINPs prepared via the traditional one-stage surface cross-linking using diazide **22** and those with the double surface-cross-linking. What we noticed was that by itself, **22** was worse than **23** and even worse than **6**, despite its C3 tether. For example, for templates 24, 25, and 26, the MINPs prepared with **22** bound its own templates with a binding constant of Ka = 1.37, 2.97, and 2.31 × 105 M-1, respectively (Table 2, entries 1, 4, and 7). These numbers were consistently lower than those for the corresponding MINPs prepared with the 4-carbon-based cross-linker **6** (Table 1, entries 6, 7, 11), let alone the 3-carbon-based **23** (Table 1, entries 1, 4, 10). We attributed the poor performance of **22** to its low water-solubility—overall, this compound is considerably more hydrophobic than the multihydroxylated **23**. As shown by the earlier data for the MINP prepared with **11**, aqueous solubility of the cross-linker is important to its reaction with the alkyne groups on the micelle and strongly affects the performance of the final MINPs.

Even though we started at a lower level for **22** as stated above, the two-stage double surface-cross-linking was very helpful. As shown in Table 2, addition of dialdehyde **27** increased the Ka values by an order of magnitude for all three templates. The changes

correspond to 1.3–1.7 kcal/mol of binding free energy, suggesting that the second surface-cross-linking was quite significant to the formation of the binding pockets.

In Table 1, when **23** was used as the surface-cross-linker, the binding (between a MINP and its own template) followed the order of **25** > **24**> **26** (Table 1, entries 1, 4, 10). In the earlier discussion, we have attributed the order to the favorable electrostatic interactions between the anionic templates (**24** and **25**) and their cationic MINPs, as well as the deeper, more hydrophobic imprinted binding pocket in case of MINP(**25**). In Table 2, when the MINPs were constructed with the two-stage double surface-cross-linking, the binding followed the order of **25** > **26** > **24**. Thus, although **25** remained superior in its imprinting and binding, the nonionic **26** overtook **24** in the doubly surface-cross-linked micelles. One likely reason is that, in the expanded imprinted pockets, the multiple hydroxyl groups from **27** might be engaged in hydrogen-bonding interactions with the hydroxylated portion of **26**. Although the expanded portion of the binding site is fairly hydrophilic being composed of functional groups from **22** and **27**, guest binding will partially desolvate the binding site, facilitating its hydrogen-bonding interactions with the template.

We also tried compound **28**, another water-soluble dialdehyde for the second surface-cross-linking but saw no improvement at all in the binding properties. It is possible that the two aldehyde groups in glyoxal were simply too close to allow the compound to bridge the alkoxyamine groups on the surface of the micelle for the second round of cross-linking.

Another improvement of the doubly surface-cross-linked MINPs was in their binding selectivity. Table 2 shows that the ratio of binding constants between **24** and **25** was 12.9/1.9 = 6.6 for MINP(**24**). This number was higher than that for MINP(**24**) prepared with **23** as the surface cross-linker (Table 1, 20.7/4.04 = 5.1). The ratio of binding constants between **25** and

24 for MINP(**25**) was 33.7/2.9 = 11.6 (Table 2), also higher than the corresponding ratio for MINP(**25**) prepared with **23** as the surface cross-linker (Table 1, 30.8/4.25 = 7.2). Compounds **24** and **25** are isomeric structures with small differences; it is encouraging that the two-stage double surface-cross-linking consistently improved the binding selectivity among highly similar structural analogues.

CHAPTER 3. EXPERIMENTAL SECTION

General Method

Routine 1H and 13C NMR spectra were recorded on a Bruker DRX-400, on a Bruker AV II 600 or on a Varian VXR-400 spectrometer. ESI-MS mass was recorded on Shimadzu LCMS-2010 mass spectrometer. Dynamic light scattering (DLS) data were recorded at 25 °C using PDDLS/ CoolBatch 90T with PD2000DLS instrument. Isothermal titration calorimetry (ITC) was performed using a MicroCal VP-ITC Microcalorimeter with Origin 7 software and VPViewer2000 (GE Healthcare, Northampton, MA). Compounds **24**, **25**, **26, 28** and 1,3-dichloroacetone were commercially available.
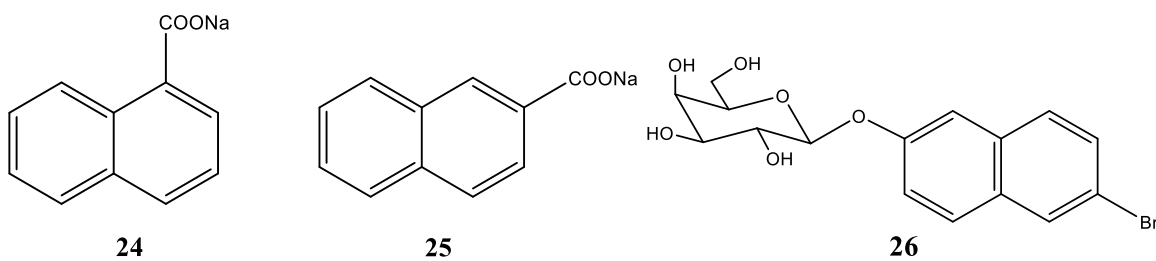
Chart 3.1 Structures of templates used in study**.**
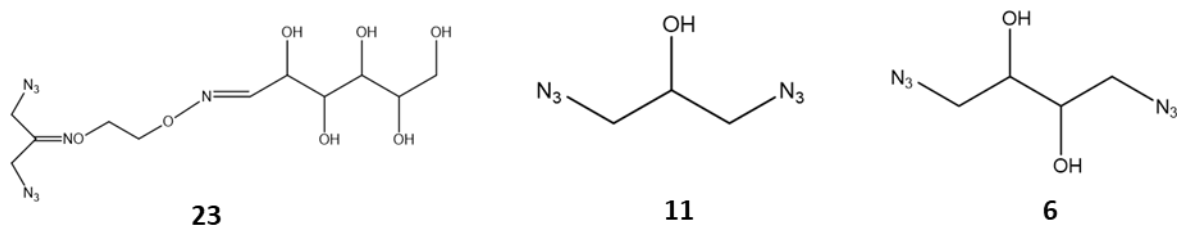

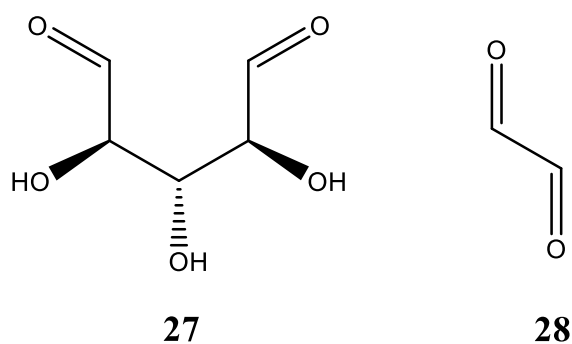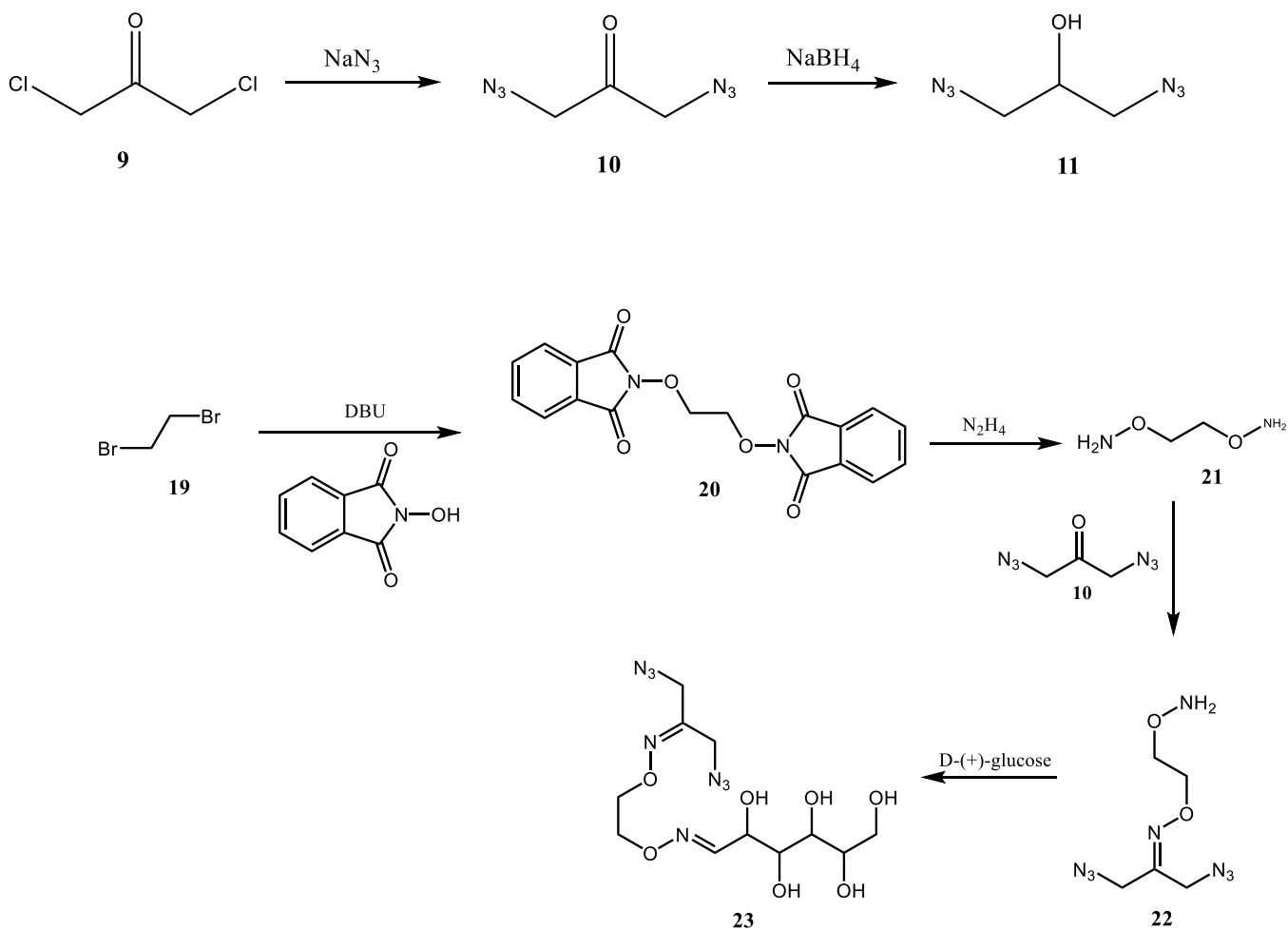Chart 3.2 Structures of cross-linkers used in study.

Chart 3.3 Structures of aldehyde-linkers used in study.

Scheme 3.1 Synthesis route for cross-linkers

Syntheses

Syntheses of compound **4**[1] and **27**[2] were previously reported.

Compound 10. Sodium azide (2.60 g, 40 mmol) was added to a solution of 1,3-dichloroacetone (1.02 g, 8 mmol) in acetone (15 mL). The reaction mixture was stirred at 25 °C for 15h. Precipitate (NaCl) was removed vacuum filtration. The residue acetone was removed by rotary evaporation to obtain compound **10** as a colorless oil (0.89g, 79%). ^{1}H NMR (400 MHz, CD$_3$OD, δ): 4.09 (s, 4H) ppm. ^{13}C NMR (100 MHz, CD$_3$OD, δ): 199.4, 55.8 ppm. ESI - HRMS calcd for C$_3$H$_4$N$_6$O (*m/z*): [M + Cl]$^-$, 175.4977; found, 175.0137.

Compound 11. To a solution of **10** (0.89 g, 6.3 mmol) in THF (30 mL), sodium borohydride (0.363 g, 9.6 mmol) in 3ml water was added slowly at 0 °C. The reaction mixture was stirred at 25 °C for 1 hour, then neutralized with 1M HCl aqueous solution and extracted with EA (3 × 30 mL). The organic phase was combined and washed with brine (2 × 30 mL), dried over sodium sulfate, filtered, and concentrated by rotary evaporation. The residue was purified by column chromatography over silica gel using 1: 1 methylene chloride/ n-hexane as eluent to afford compound **12** as a colorless oil (0.72 g, 80 %). ^{1}H NMR (400 MHz, CCl$_3$D, δ): 3.93 (p, *J* = 6.0 Hz, 1H), 3.41 (m, 4H), 2.42 (s, 1H) ppm. ^{13}C NMR (100 MHz, CCl$_3$D, δ): 69.6, 53.9 ppm. ESI - HRMS calcd for C$_3$H$_6$N$_6$O (*m/z*): [M + Na]$^+$, 165.0500; found, 165.1133.

Compound 22. To a solution of N-hydroxyphthalimide (10.47 g, 64.2 mmol) in DMF (70 mL), 1,8-diazabicyclo[5.4.0]undec-7-ene (9.78 g, 64.2 mmol) and 1,2-dibromoethane (6.03 g, 32.1 mmol) were added. The reaction mixture was stirred at 80 °C for 4 hours, and cooled to room temperature. The resulting solution was poured into ice and the precipitate was filtered and washed with cold water (30ml) followed by cold CH$_3$CN (30 ml). The crude 1,2-diphthalimidooxyethae was dissolved into 30 mL ethanol, followed by addition of hydrazine hydrate aqueous solution (35 wt%, 8.805 g, 96.3 mmol). The reaction mixture was stirred at 25 °C overnight. Then the solvent was removed by rotary evaporation and added DCM (35ml)

[1] Awino, J. K.; Zhao, Y. *J. Am. Chem. Soc.* **2013**, *135*, 12552.

[2] Shankar, B.B.; Kirkup, M.P.; McCombie, S.W.; Ganguly, A.K. *Tetrahedron. Letters.* **1993**, 34, 45, 7171

to the residue white solid. Let the solution stand for 12 hours. Then removed the precipitate by vacuum filtration. The solvent was removed by rotary evaporation to obtain colorless oil. The colorless oil and **10** (8.99 g, 64.2 mmol) were added into 30ml ethanol and the reaction mixture was stirred at 50 °C for 24 hours. Removed the solvent by rotary evaporation and the residue was purified by column chromatography over silica gel using 1: 2 ethyl acetate/ n-hexane as eluent to afford compound **10** as a colorless oil (1.72 g, 25 %). ^{1}H NMR (600 MHz, CCl$_3$D, δ): 5.50 (s, 2H), 4.34 (t, *J* = 6.0 Hz, 2H), 4.27 (s, 2H), 4.00 (s, 2H), 3.92 (t, *J* = 6.0 Hz, 2H) ppm. ^{13}C NMR (150MHz, CCl$_3$D, δ): 150.6, 73.6, 72.7, 51.1, 45.7 ppm. ESI - HRMS calcd for C$_5$H$_{10}$N$_8$O$_2$ (*m/z*): [M + H]$^+$, 215.0927; found, 215.0996.

Compound 23. Dissolved 10 (437.0 mg, 2.1 mmol) and D-(+) Glucose (1875.0 mg, 10.5 mmol) in 30 ml methanol and water (3/1, v/v). And the reaction mixture was stirred at 50 °C for 24 hours. Removed the solvent by rotary evaporation and followed by addition of 30 ml acetone and methanol (3/1, v/v). Let the solution stand overnight. The precipitate was removed by vacuum filtration. Removed the solvent by rotary evaporation to obtain pale yellow oil and added 30 ml dry DCM. Let the solution stand at -20 °C for 30 mins. Poured out the solvent slowly with precipitate left in the flask. Repeated this rinsing process for another two times to obtain colorless oil (710.6 mg, 90 %, E / Z=4 / 1). ^{1}H NMR (400 MHz, D$_2$O, δ): 7.42 (d, *J* = 8.0 Hz, 1H), 4.23 (m, 5H), 4.16 (s, 2H), 3.97 (s, 2H), 3.81 (d, *J* = 8.0 Hz, 1H), 3.65 (m, 2H), 3.47 (m, 2H) ppm. ^{13}C NMR (100 MHz, D$_2$O, δ): 153.5, 152.6, 151.5, 72.8, 72.5, 72.3, 71.9, 71.0, 70.8, 70.7, 70.7, 70.3, 70.1, 69.9, 66.3, 62.8, 62.6, 50.7, 50.7, 45.9, 45.8 ppm. ESI - HRMS calcd for C$_{11}$H$_{20}$N$_8$O$_7$ (*m/z*): [M + H]$^+$, 377.1455; found, 377.1526.

Typical Procedure for the Synthesis of Functionalized MINPs.

(a) Preparation of MINP: a micellar solution of surfactant **4** (9.3 mg, 0.02 mmol) in H$_2$O (2.0 mL) was added to the above complex, followed by the addition of DVB (2.8 μL, 0.02 mmol), and DMPA in DMSO (10 μL of a 12.8 mg/mL solution, 0.0005mmol). The mixture was subjected to ultrasonication for 10 min before cross-linker **23** (9.1 mg, 0.024mmol), CuCl$_2$ in H$_2$O (10 μL of 6.7 mg/mL solution, 0.0005 mmol), and sodium ascorbate in H$_2$O (10 μL of 99 mg/mL solution, 0.005 mmol) were added. After the reaction mixture was stirred slowly at room temperature for 12 hours, linear sugar **5** (10.6 mg, 0.04 mmol), CuCl$_2$ in H$_2$O (10 μL of 6.7 mg/mL solution, 0.0005 mmol), and sodium ascorbate in H$_2$O (10 μL of 99 mg/mL

solution, 0.005 mmol) were added. The mixture was stirred at room temperature for another 6 hours, purged with nitrogen for 15 min, sealed with a rubber stopper, and irradiated in a Rayonet reactor for 12 hours. The progress of reaction could be monitored by ^{1}H NMR spectroscopy and dynamic light scattering (DLS). The reaction mixture was poured into acetone (8 mL). The precipitate collected by centrifugation was washed with a mixture of acetone/water (5 mL/1 mL) three times, followed by methanol/acetic acid (5 mL/0.1 mL) three times. The solid was then rinsed two times with acetone (5 mL) and dried in air to afford the final MINPs. Typical yields were >80%.

(b) Preparation of surface cross-linking MINP: a micellar solution of surfactant **4** (9.3 mg, 0.02 mmol) in H_2O (2.0 mL) was added to the above complex, followed by the addition of DVB (2.8 μL, 0.02 mmol), and DMPA in DMSO (10 μL of a 12.8 mg/mL solution, 0.0005mmol). The mixture was subjected to ultrasonication for 10 min before compound **22** (5.1 mg, 0.024mmol), $CuCl_2$ in H_2O (10 μL of 6.7 mg/mL solution, 0.0005 mmol), and sodium ascorbate in H_2O (10 μL of 99 mg/mL solution, 0.005 mmol) were added. After the reaction mixture was stirred slowly at room temperature for 12 hours, linear sugar **5** (10.6 mg, 0.04 mmol), $CuCl_2$ in H_2O (10 μL of 6.7 mg/mL solution, 0.0005 mmol), and sodium ascorbate in H_2O (10 μL of 99 mg/mL solution, 0.005 mmol) were added. The mixture was stirred at room temperature for another 6 hours, purged with nitrogen for 15 min, sealed with a rubber stopper, and irradiated in a Rayonet reactor for 12 hours. Then aniline (2.19 μL, 2.2 mg, 0.024 mmol) and compound **27** (1.8 mg, 0.012 mmol) were added. The mixture was stirred at 60 °C for 24 hours. The progress of reaction could be monitored by ^{1}H NMR spectroscopy and dynamic light scattering (DLS). The reaction mixture was poured into acetone (8 mL). The precipitate collected by centrifugation was washed with a mixture of acetone/water (5 mL/1 mL) three times, followed by methanol/acetic acid (5 mL/0.1 mL) three times. The solid was then rinsed two times with acetone (5 mL) and dried in air to afford the final MINPs. Typical yields were >80%.
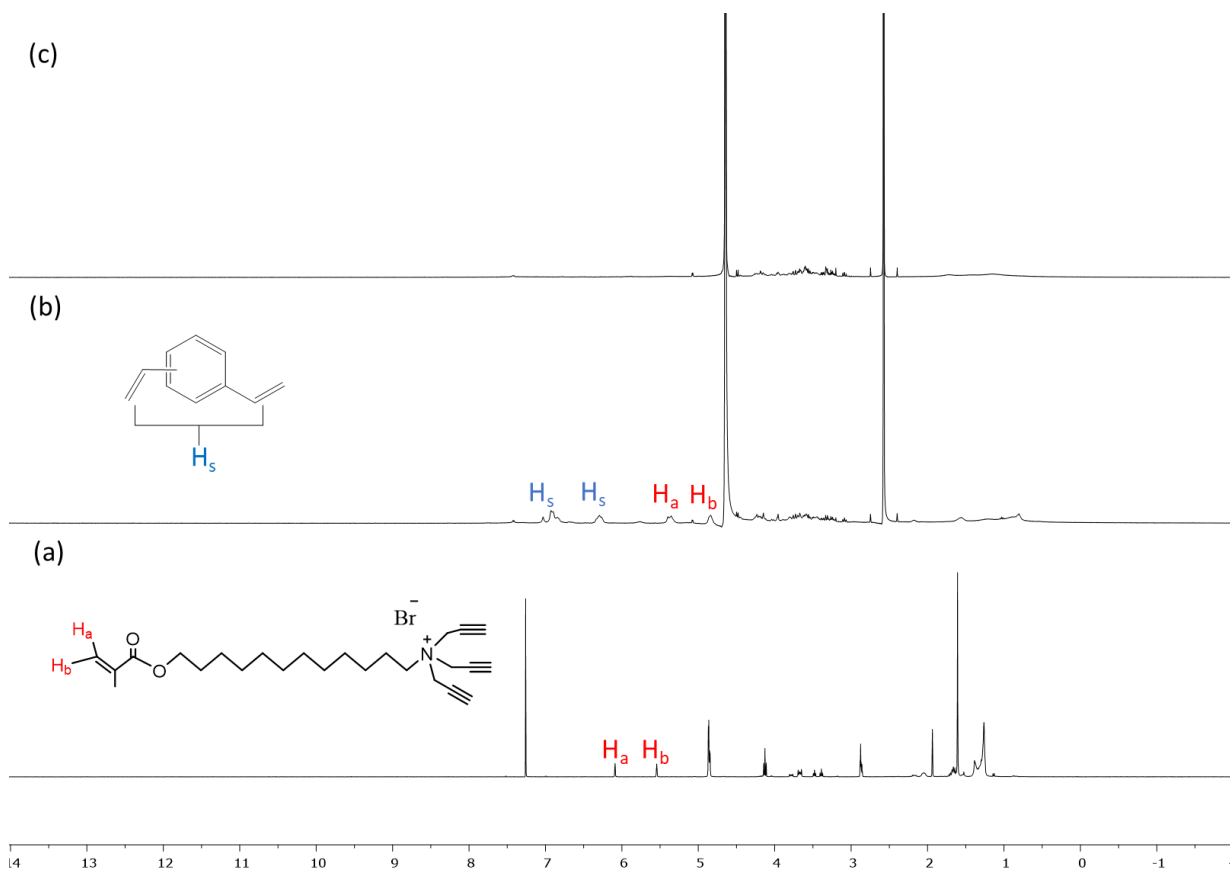
Figure 3.1 ^{1}H NMR spectra of (a) **4** in CDCl$_3$, (b) alkynyl-SCM in D$_2$O, and (c) MINP made with cross-linker **6** in D$_2$O.
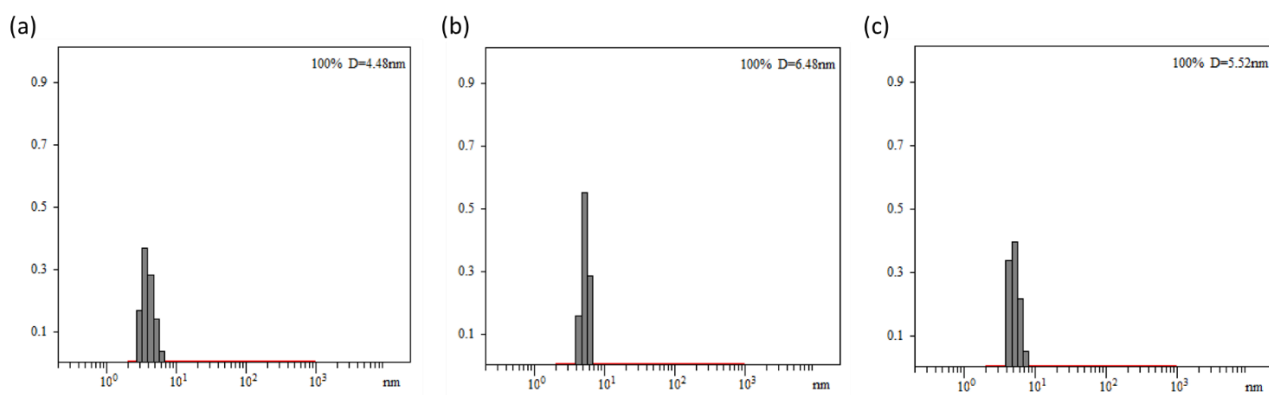

Figure 3.2 Distribution of the hydrodynamic diameters of the nanoparticles in water as

determined by DLS for (a) alkynyl-SCM, (b) surface-functionalized SCM, and (c) MINP made
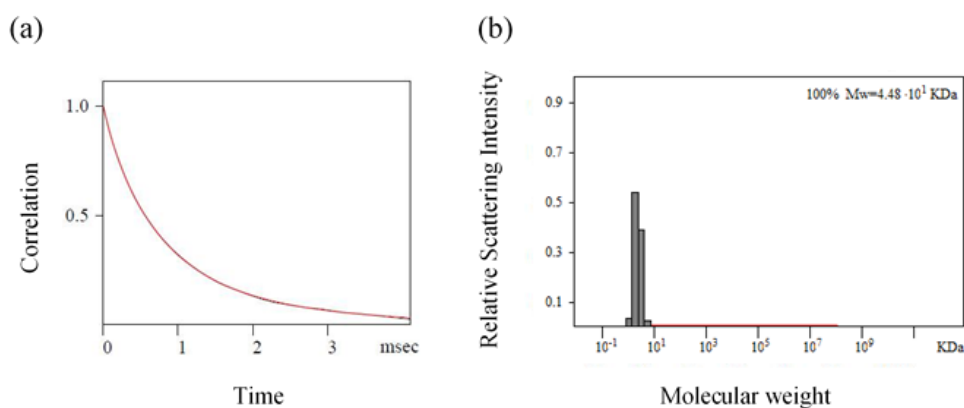with cross-linker **6** in water.

Figure 3.3 The correlation curve and the distribution of the molecular weight for MINP from
the DLS. The PRECISION DECONVOLVE program assumes the intensity of scattering is
proportional to the mass of the particle squared. If each unit of building block for the MINP is
assumed to contain one molecule of compound **4** (MW = 465 g/mol), 1.2 molecules of
compound **6** (MW = 172 g/mol), one molecule of DVB (MW = 130 g/mol) and 0.8 molecules
of compound **5** (MW =264 g/mol), the molecular weight of MINP made with compound **6**
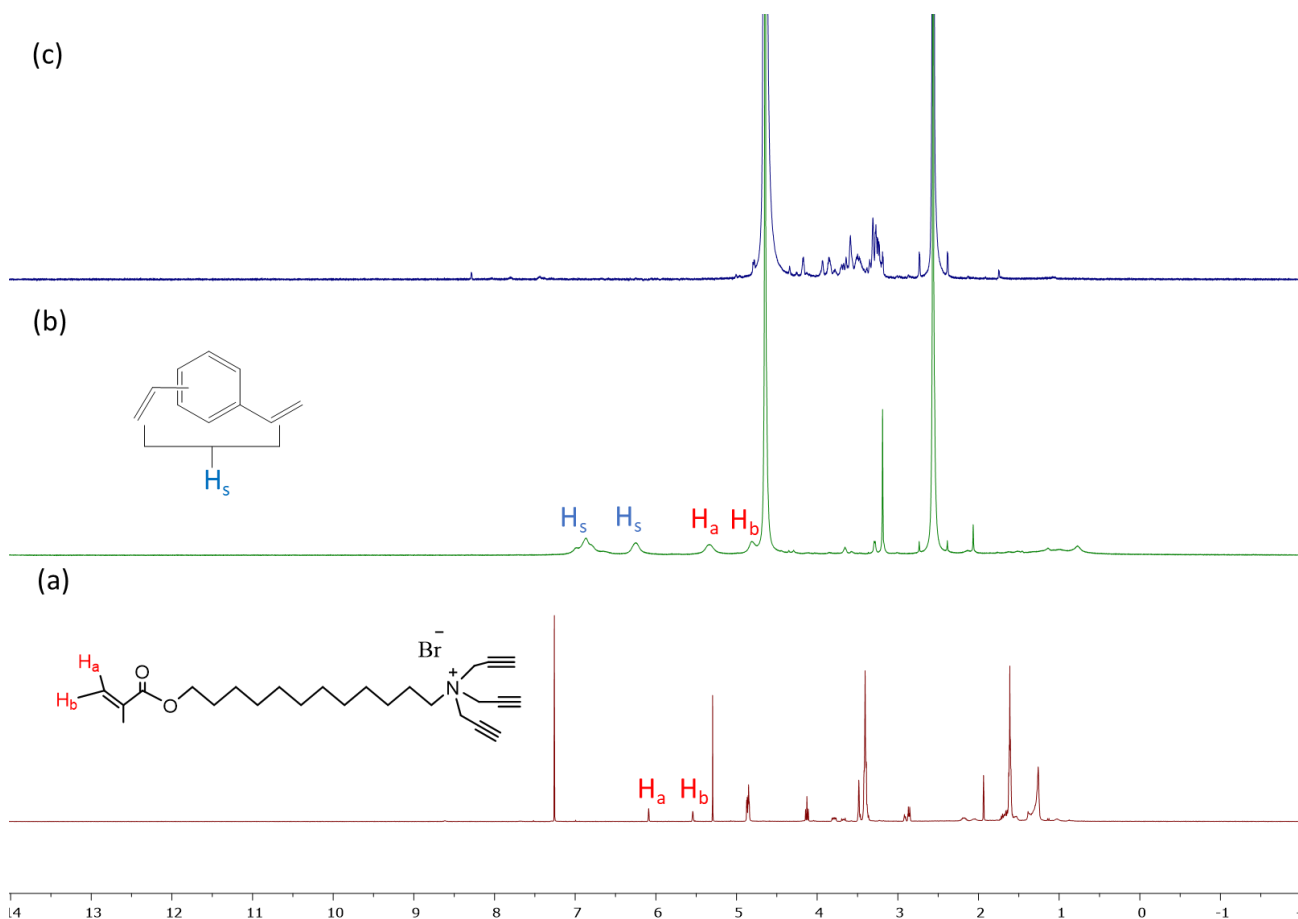translates to 44 [= 44800 / (465 + 1.2×172 + 130 + 0.8×264)] of such units.

Figure 3.4 ^{1}H NMR spectra of (a) **4** in CDCl$_3$, (b) alkynyl-SCM in D$_2$O, and (c) MINP made with cross-linker **11** in D$_2$O.
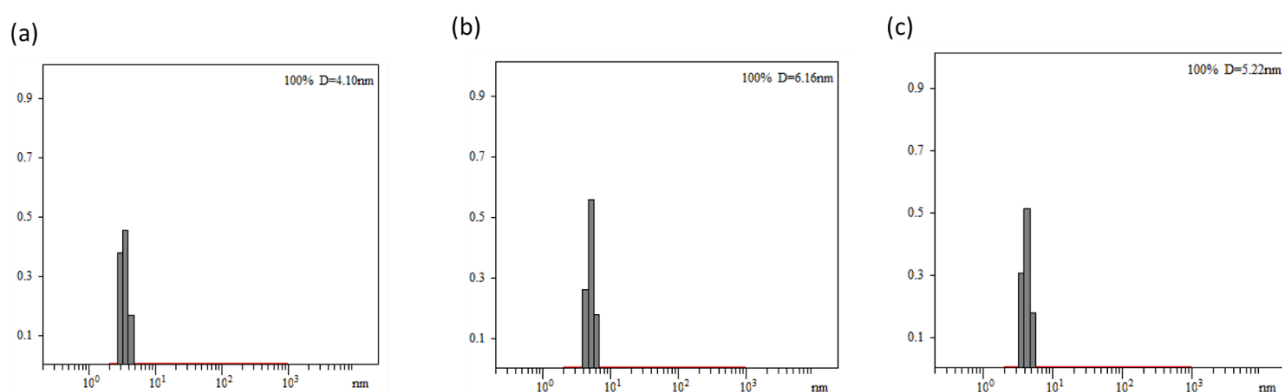

Figure 3.5 Distribution of the hydrodynamic diameters of the nanoparticles in water as determined by DLS for (a) alkynyl-SCM, (b) surface-functionalized SCM, and (c) MINP made with cross-linker **11** in water in water.
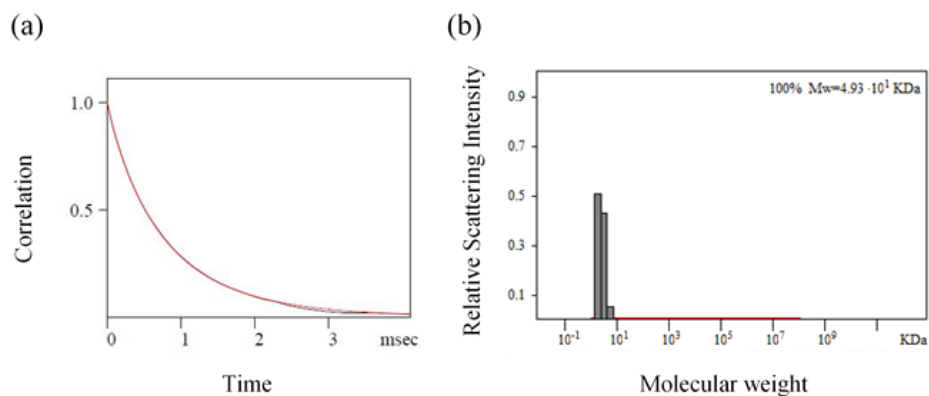
Figure 3.6 The correlation curve and the distribution of the molecular weight for MINP from the DLS. The PRECISION DECONVOLVE program assumes the intensity of scattering is proportional to the mass of the particle squared. If each unit of building block for the MINP is assumed to contain one molecule of compound **4** (MW = 450 g/mol), 1.2 molecules of compound **11** (MW = 142 g/mol), one molecule of DVB (MW = 130 g/mol) and 0.8 molecules of compound **5** (MW =264 g/mol), the molecular weight of MINP made with compound **6** translates to 50 [= 49300 / (465 + 1.2×142 + 130 + 0.8×264)] of such units.
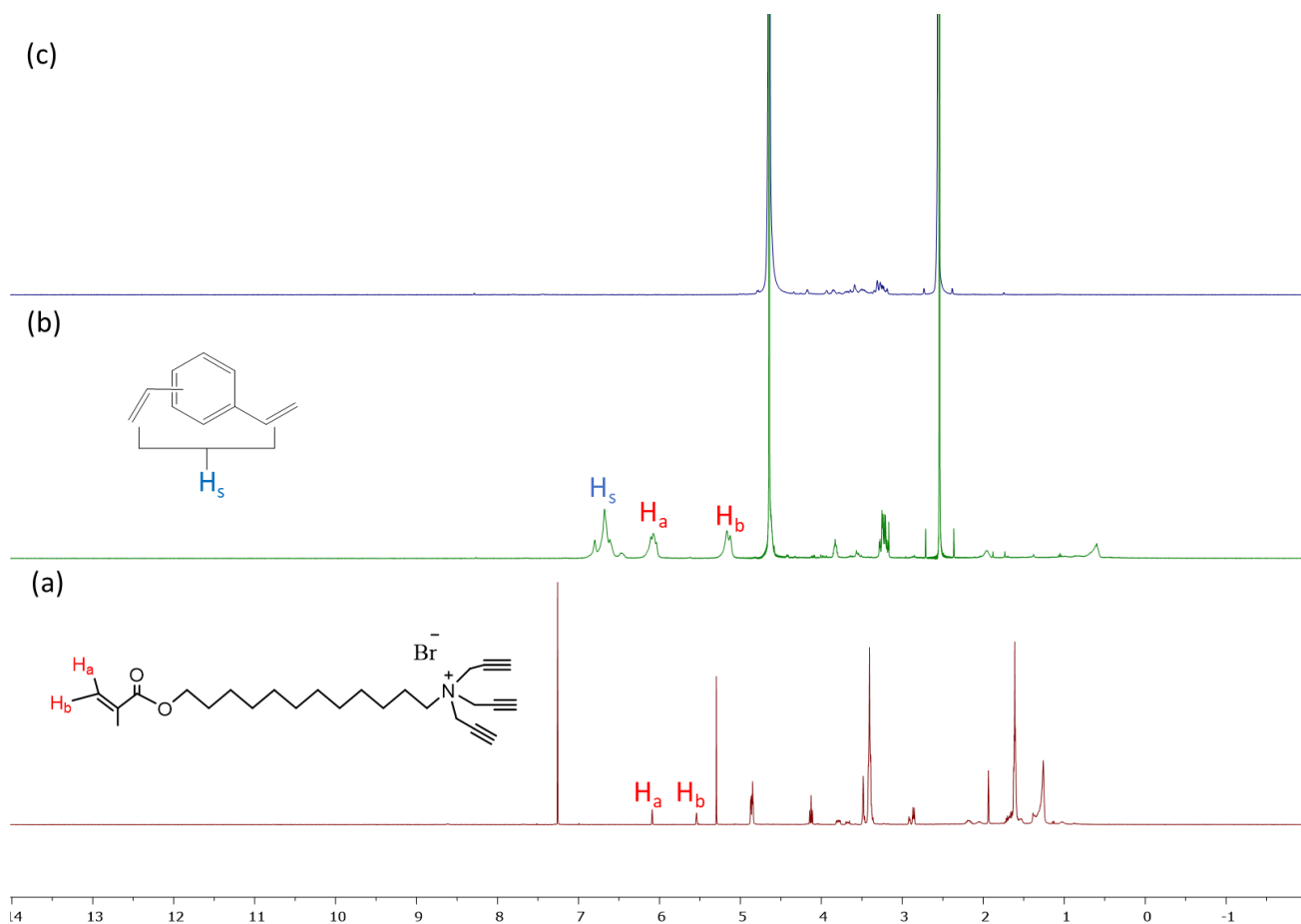
Figure 3.7 ^{1}H NMR spectra of (a) **3** in CDCl$_3$, (b) alkynyl-SCM in D$_2$O, and (c) MINP made with cross-linker **22** with in D$_2$O.
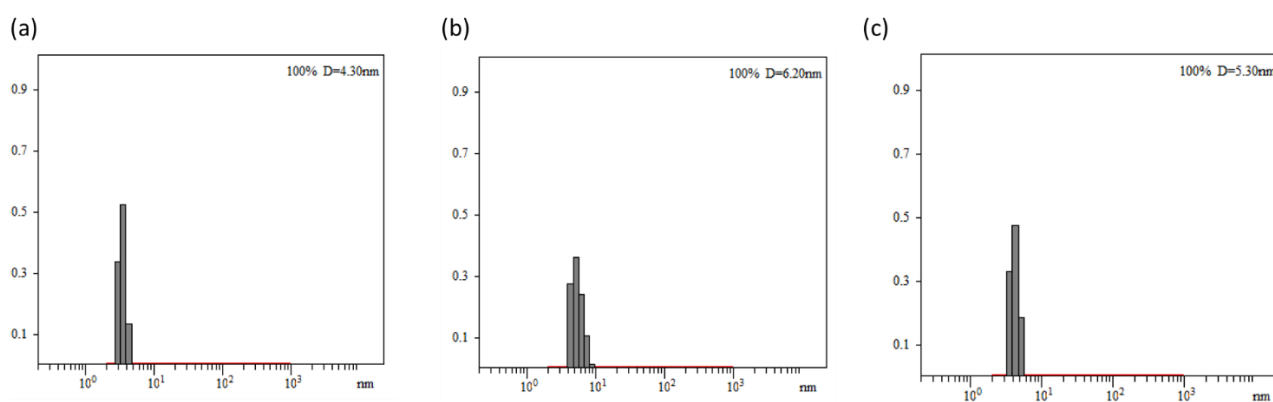

Figure 3.8 Distribution of the hydrodynamic diameters of the nanoparticles in water as determined by DLS for (a) alkynyl-SCM, (b) surface-functionalized SCM, and (c) MINP made with cross-linker **22** in water.
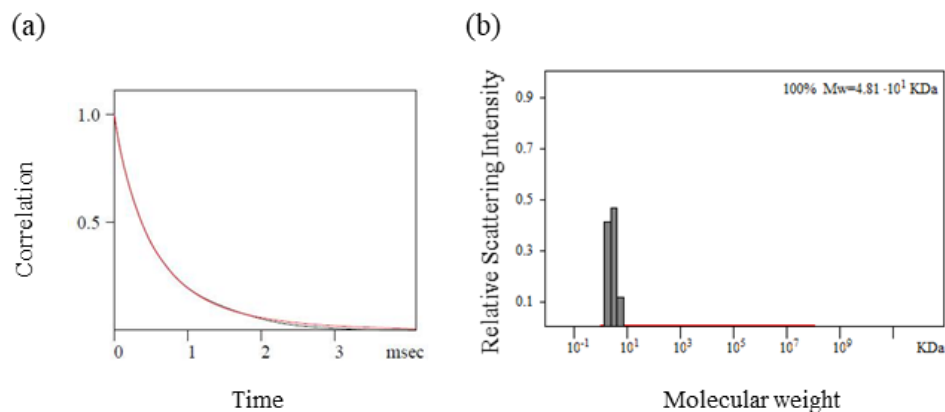
Figure 3.9 The correlation curve and the distribution of the molecular weight for MINP from the DLS. The PRECISION DECONVOLVE program assumes the intensity of scattering is proportional to the mass of the particle squared. If each unit of building block for the MINP is assumed to contain one molecule of compound **4** (MW = 450 g/mol), 1.2 molecules of compound **22** (MW = 214 g/mol), one molecule of DVB (MW = 130 g/mol) and one molecule of compound **5** (MW =264 g/mol), the molecular weight of MINP made with compound **6** translates to 45 [= 48100 / (465 + 1.2×214 + 130 + 0.8×264)] of such units.
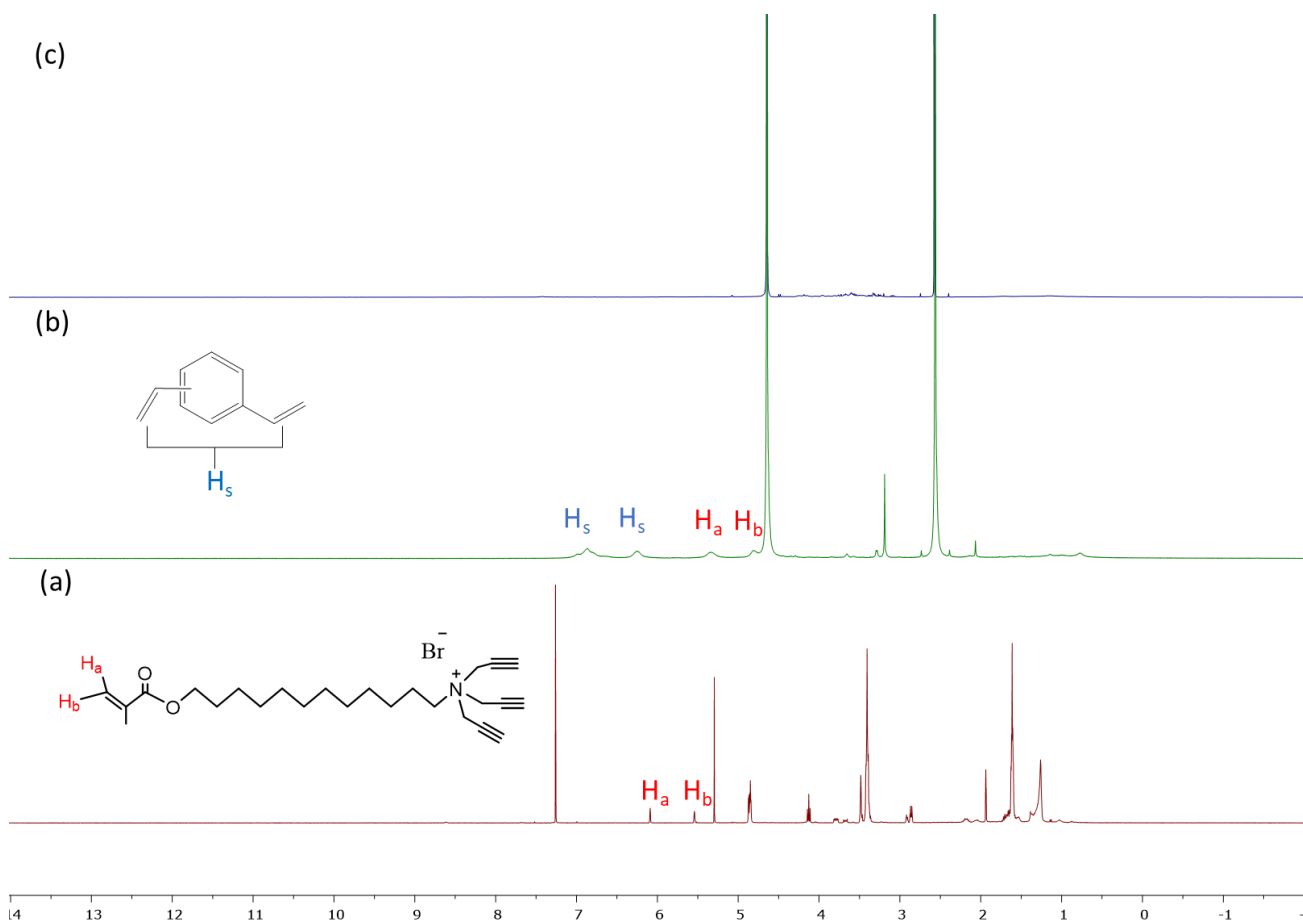
Figure 3.10 ^{1}H NMR spectra of (a) **3** in CDCl$_3$, (b) alkynyl-SCM in D$_2$O, and (c) MINP (made with cross-linker **23**) with in D$_2$O.
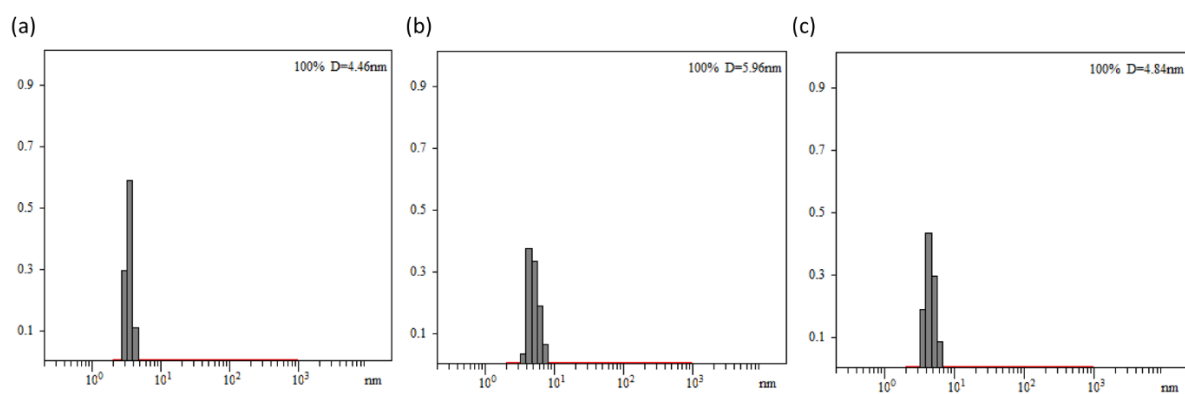

Figure 3.11 Distribution of the hydrodynamic diameters of the nanoparticles in water as determined by DLS for (a) alkynyl-SCM, (b) surface-functionalized SCM, and (c) MINP made with cross-linker **23** in water.
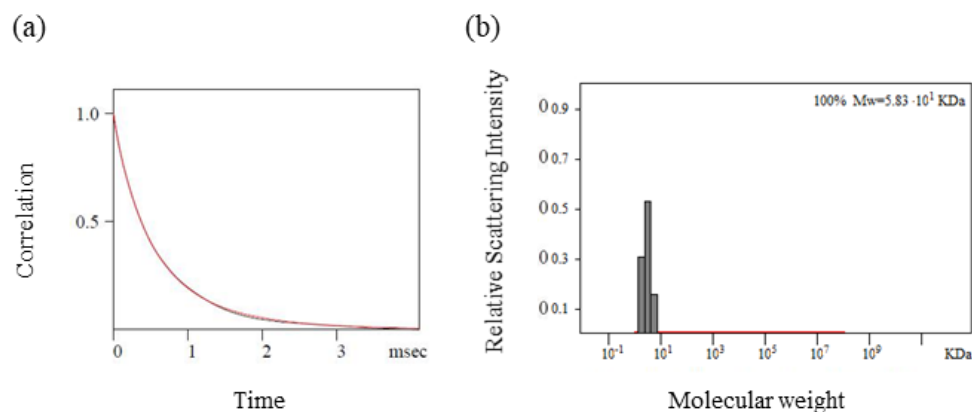
Figure 3.12 The correlation curve and the distribution of the molecular weight for MINP from the DLS. The PRECISION DECONVOLVE program assumes the intensity of scattering is proportional to the mass of the particle squared. If each unit of building block for the MINP is assumed to contain one molecule of compound **4** (MW = 450 g/mol), 1.2 molecules of compound **23** (MW = 376 g/mol), one molecule of DVB (MW = 130 g/mol) and one molecule of compound **5** (MW =264 g/mol), the molecular weight of MINP made with compound **6** translates to 46 [= 58300 / (465 + 1.2×376 + 130 + 0.8×264)] of such units.
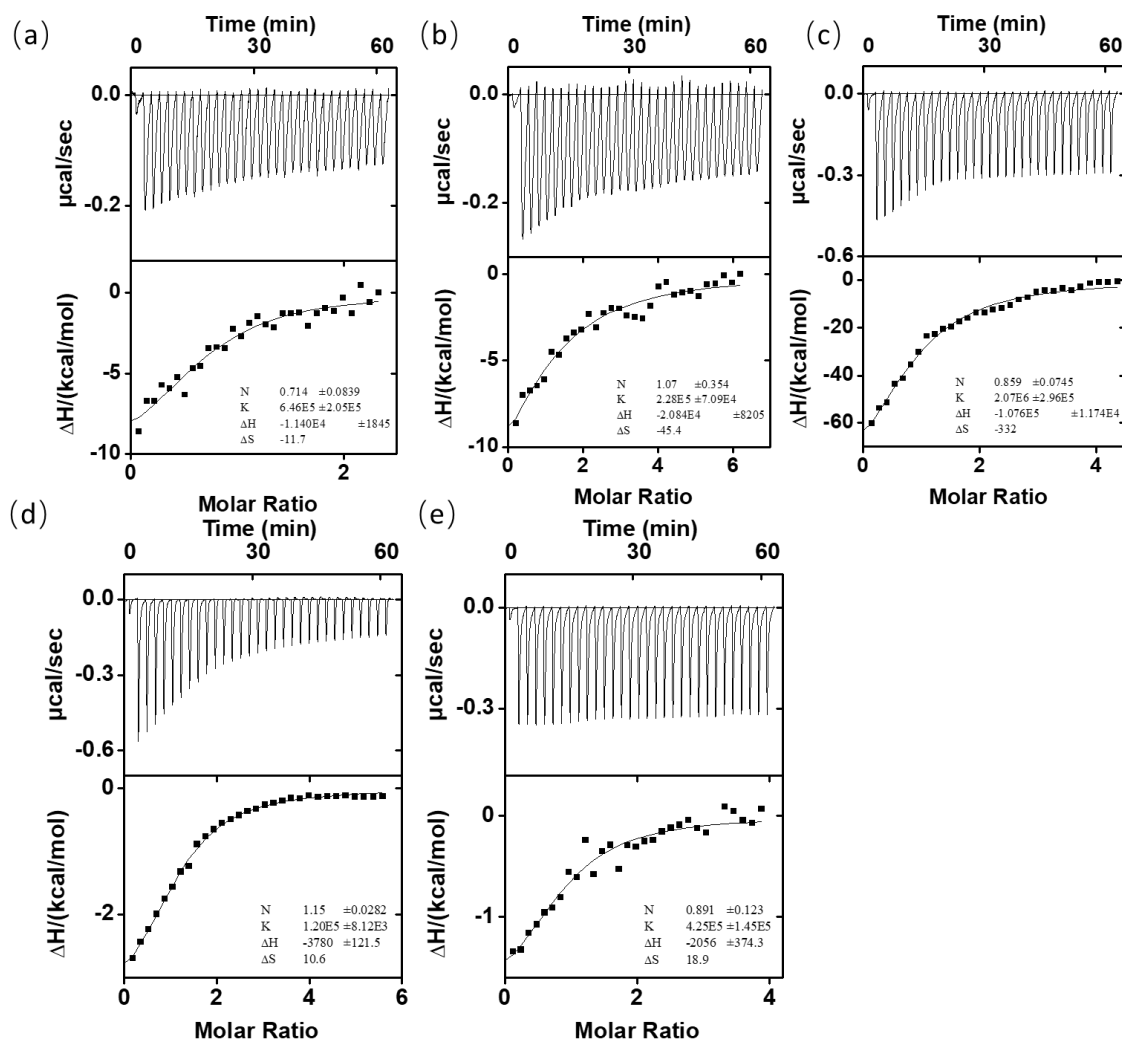
Figure 3.13 ITC titration curves obtained at 298 K for the titration of 10 μM of (a) MINP(**24**) made with compound **6**, (b) MINP(**24**) made with compound **11**, (c) MINP(**24**) made with compound **23**, (d) MINP(**25**) made with compound **6** and (e) MINP(**25**) made with compound **23** by compound **24** in 50 mM Tris Buffer (PH=7.3). The guest concentrations are (a) 120 μM, (b) 100 μM, (c) 100 μM, (d) 200 μM and (e) 200 μM, respectively. The data correspond to entries 3, 2, 1, 9, 8, respectively, in Table 2.1.

(a) Time (min)
0   30   60
µcal/sec
0.0
-0.3
ΔH/(kcal/mol)
0
-3
-6
N   0.737 ±0.0803
K   1.25E5 ±1.41E4
ΔH   -1.486E4   ±1957
ΔS   -26.5
0   2   4
Molar Ratio

(b) Time (min)
0   30   60
µcal/sec
0.0
-0.3
-0.6
ΔH/(kcal/mol)
0
-3
-6
N   1.12   ±0.0536
K   4.04E5 ±1.15E5
ΔH   -5305 ±416.8
ΔS   7.86
0   2
Molar Ratio

(c) Time (min)
0   30   60
µcal/sec
0.0
-0.6
-1.2
-1.8
-2.4
ΔH/(kcal/mol)
0
-10
-20
N   1.02   ±0.00782
K   7.59E5 ±5.57E4
ΔH   -2.057E4   ±211.0
ΔS   -42.1
0   2
Molar Ratio

(e) Time (min)
0   30   60
µcal/sec
0.0
-0.8
-1.6
-2.4
ΔH/(kcal/mol)
0
-60
-120
N   1.08   ±0.0144
K   3.08E6 ±2.99E5
ΔH   -1.033E5   ±1837
ΔS   -317
0   2
Molar Ratio
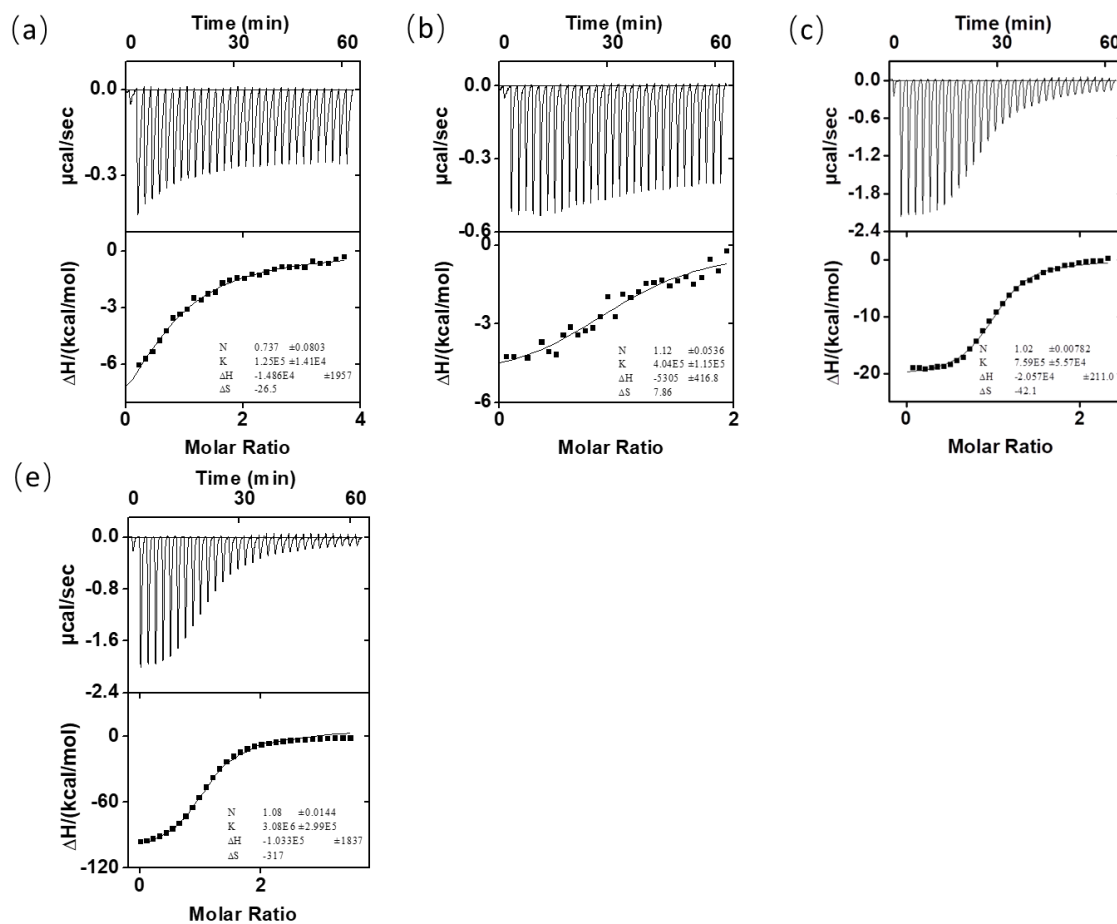
Figure 3.14 ITC titration curves obtained at 298 K for the titration of 10 µM of (a) MINP(**24**) made with compound **6**, (b) MINP(**24**) made with compound **23**, (c) MINP(**25**) made with compound **6** and (d) MINP(**25**) made with compound **23** by compound **25** in 50 mM Tris Buffer (PH=7.3). The guest concentrations are (a) 100 µM, (b) 100 µM, (c) 200 µM and (d) 200 µM, respectively. The data correspond to entries 5, 4, 7, 6, respectively, in Table 2.1.
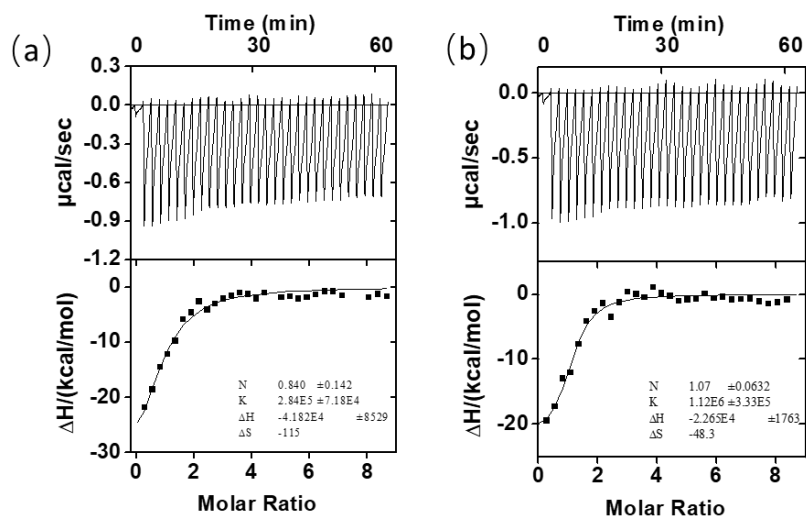
Figure 3.15 ITC titration curves obtained at 298 K for the titration of 20 μM of (a) MINP(**12**) made with compound **2** and (b) MINP(**12**) made with compound **5** by compound **12** in 50 mM Tris Buffer (PH=7.3). The guest concentrations are (a) 224 μM and (b) 224 μM respectively. The data correspond to entries 11, 10, respectively, in Table 2.1.
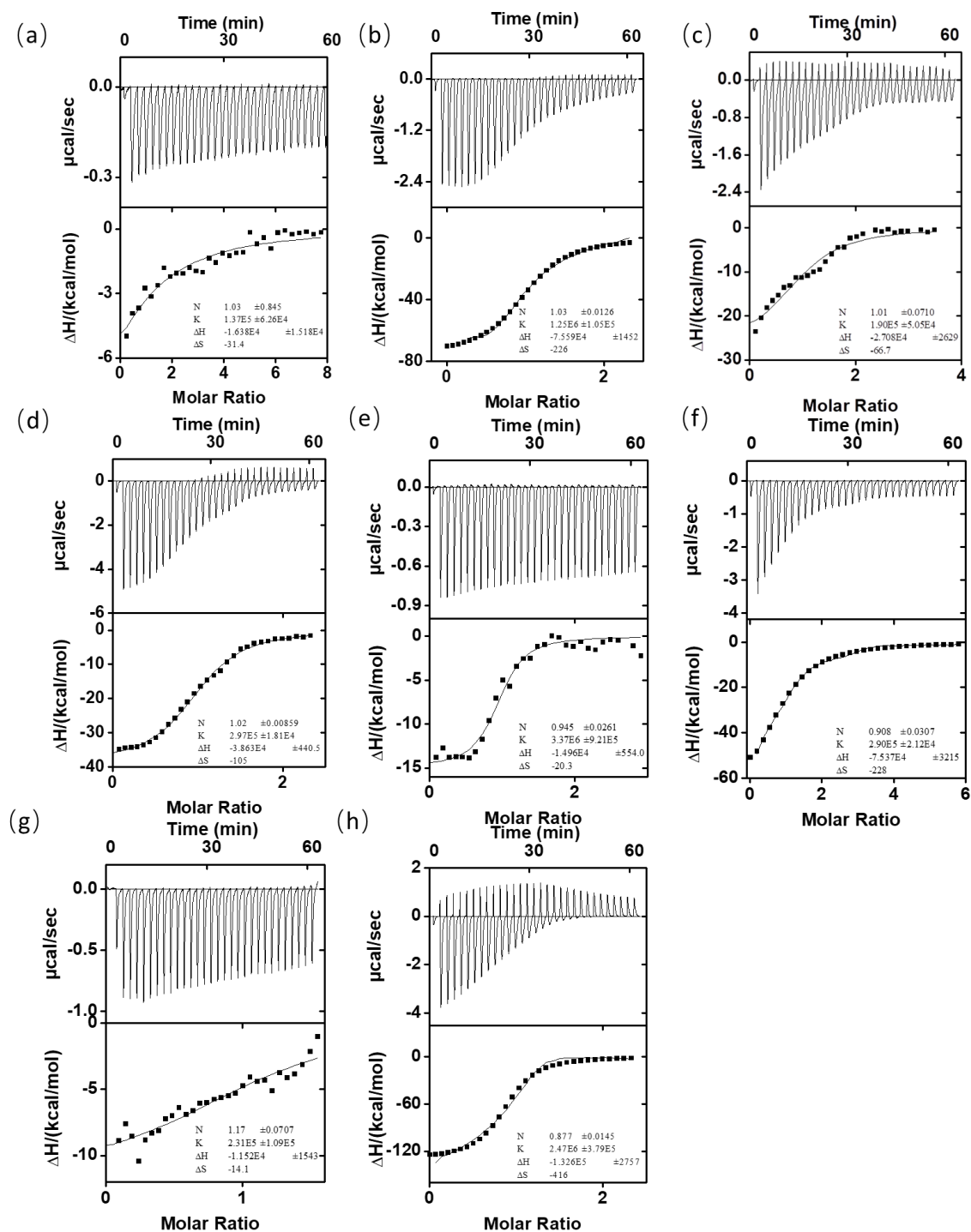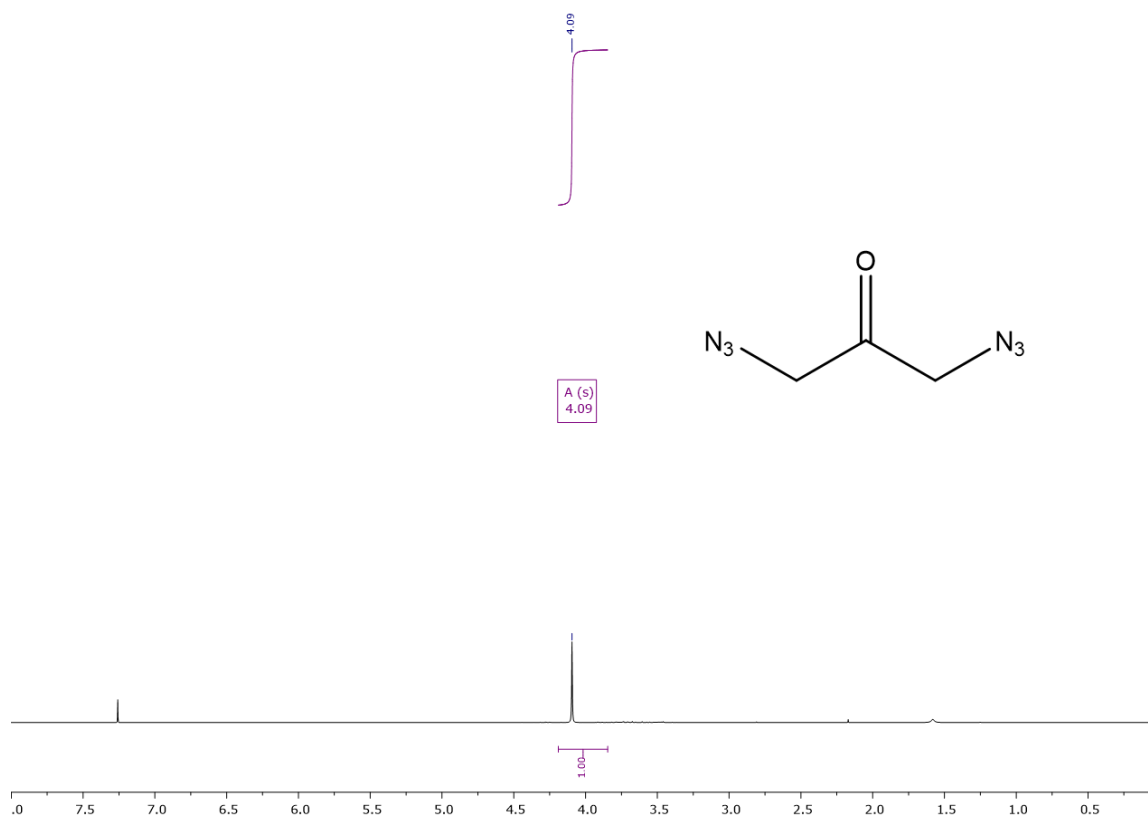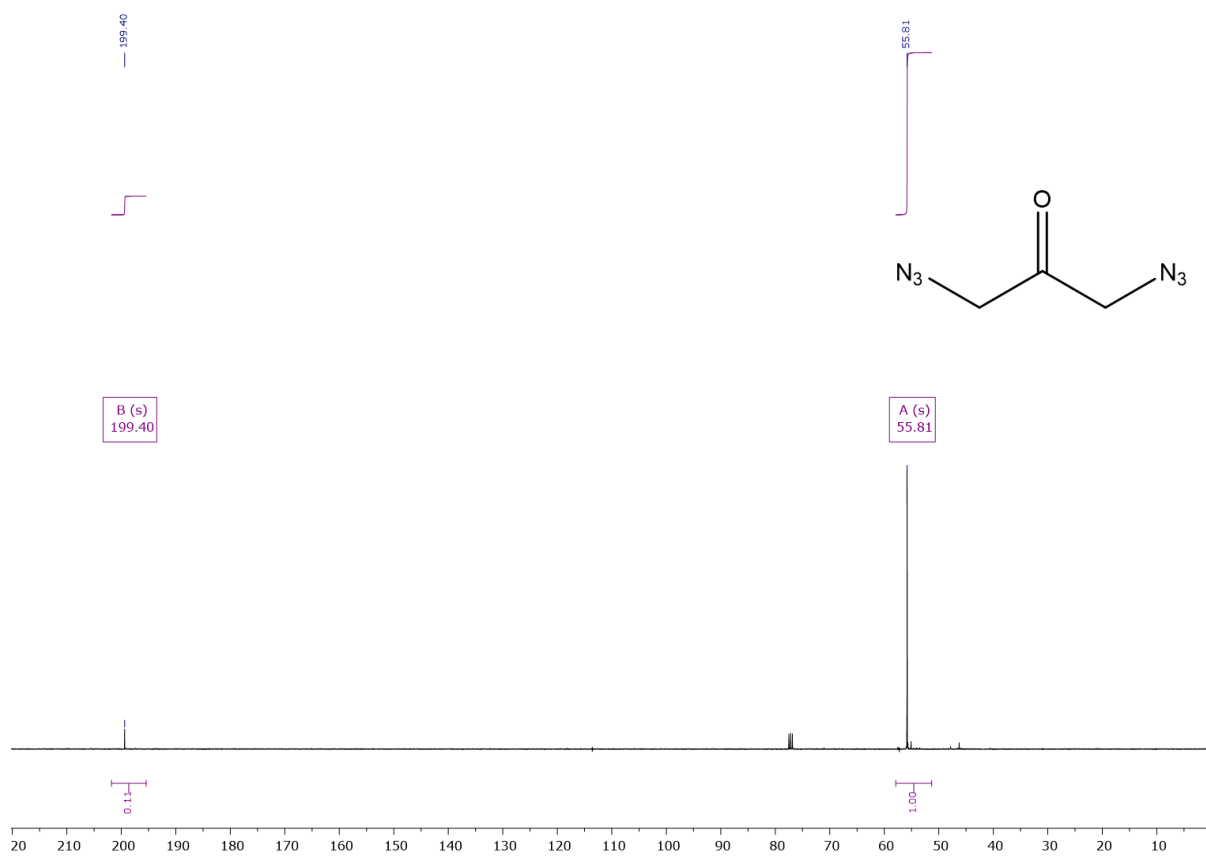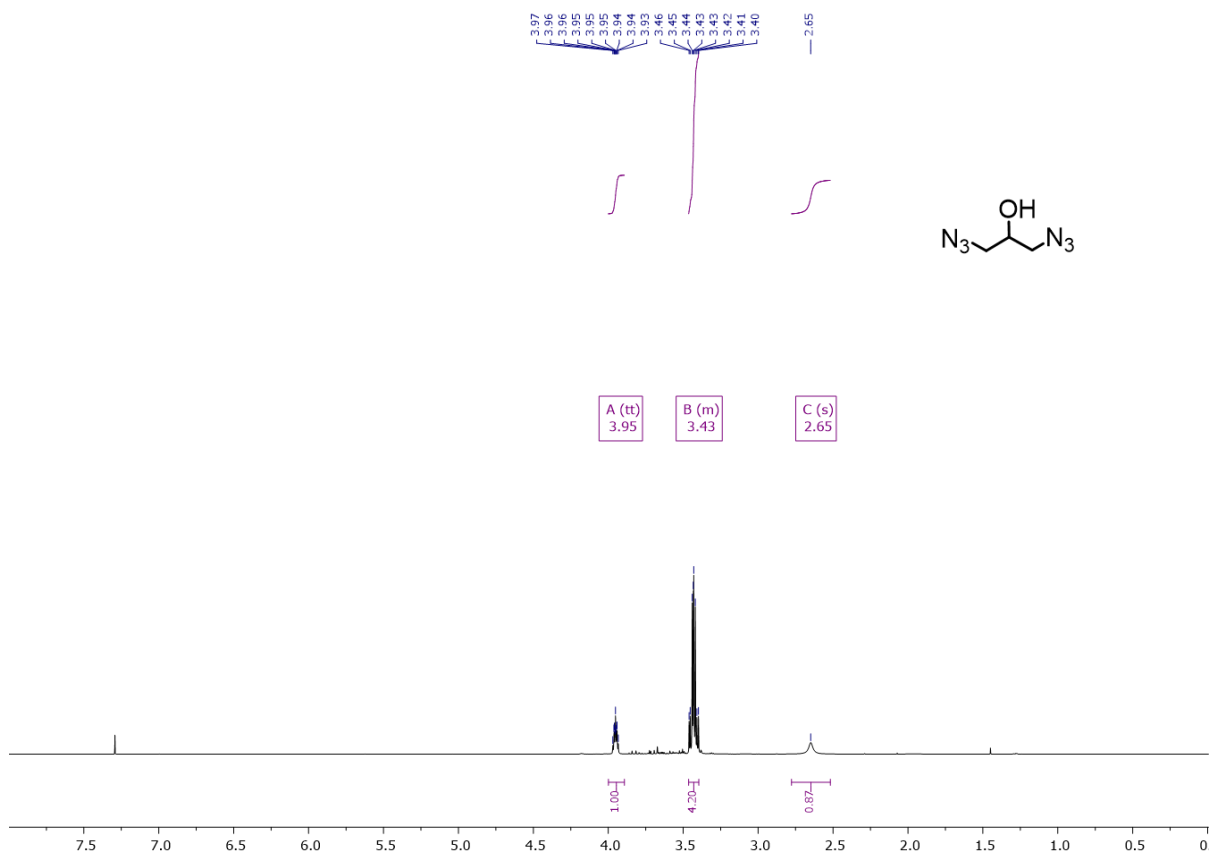
Figure 3.16 ITC titration curves obtained at 298 K for the titration of 20 μM of (a) MINP(**24**) made with compound **22** by compound **27**, (b) MINP(**24**) made with compound **22** and **27** by compound **24**, (c) MINP(**24**) made with compound **22** and **27** by compound **25**, (d) MINP(**25**) made with compound **22** by compound **25**, (e) MINP(**25**) made with compound **22** and **27** by

compound **25**, (f) MINP(**25**) made with compound **22** and **27** by compound **24**, (g) MINP(**26**) made with compound **22** and (h) MINP(**26**) made with compound **22** and **27** by compound **26** in 50 mM Tris Buffer (PH=7.3). The guest concentrations are (a) 200 μM, (b) 100 μM, (c) 200 μM, (d) 100 μM, (e) 100 μM, (f) 200 μM, (g) 224 μM, (h) 224 μM, respectively. The data correspond to entries 1, 2, 3, 4, 5, 6, 7, 8, respectively, in Table 2.2.

^{1}H & ^{13}C NMR spectra

199.40

55.81

B (s)
199.40

A (s)
55.81

O

N₃

N₃

0.1

1.00

20 210 200 190 180 170 160 150 140 130 120 110 100 90 80 70 60 50 40 30 20 10

A (tt) 3.95 | B (m) 3.43 | C (s) 2.65

A (s)
69.60

B (s)
53.87

A (s)
5.50

E (m)   C (s)
4.34   4.00

B (s)   D (m)
4.27   3.92

150.60

73.60
72.66

51.08
45.70

A (s)
150.60

C (s)
72.66

B (s)
73.60

E (s)
45.70

D (s)
51.08

170 160 150 140 130 120 110 100 90 80 70 60 50 40 30 20 10 0

1.00

4.69
4.04

5.73

4.45
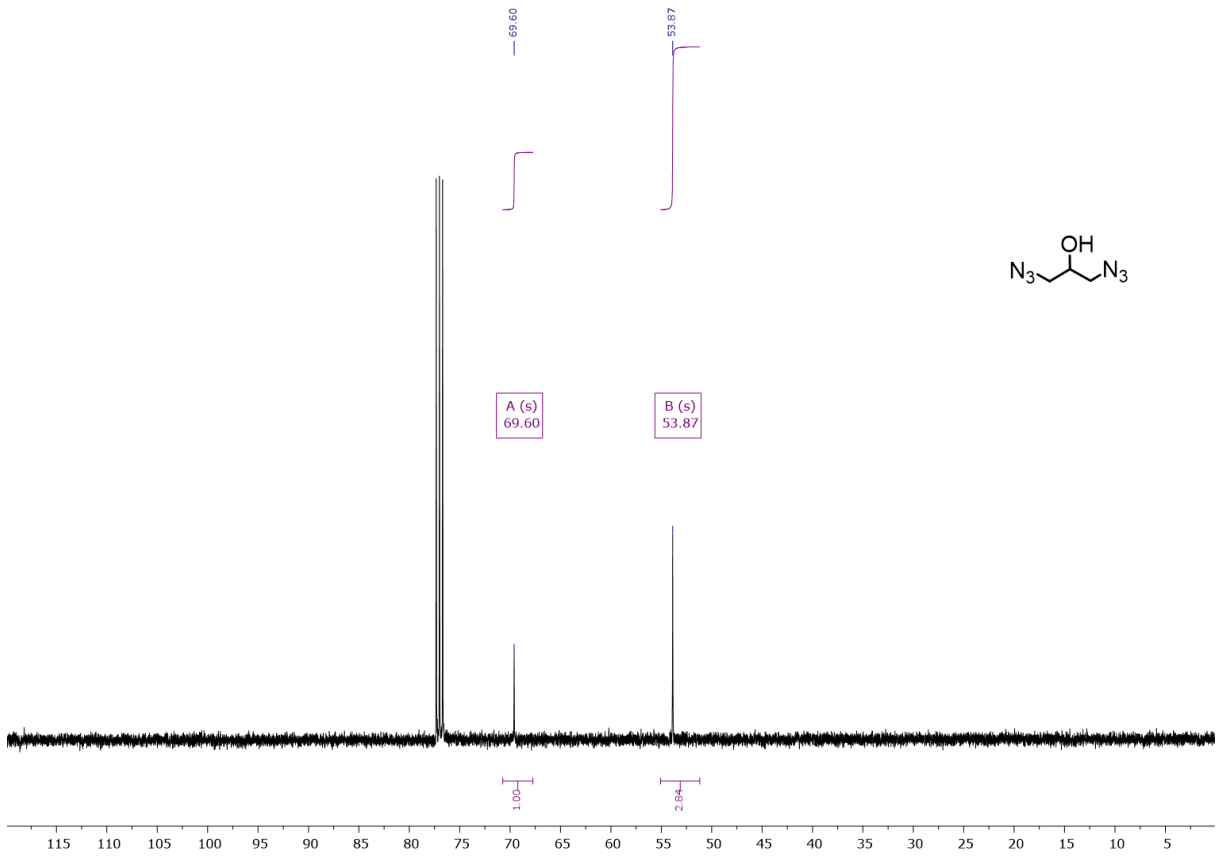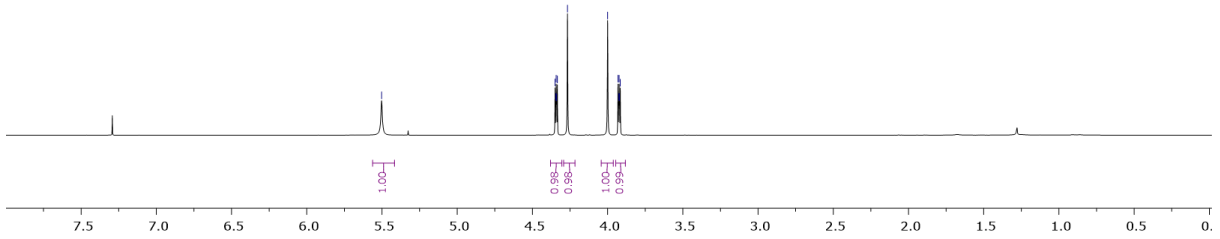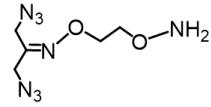
CHAPTER 4. CONCLUSION

Even though selective molecular recognition in water is considered highly challenging due to the compromise of hydrogen bonds by solvent competition,[62] the molecularly imprinted cross-linked micelle is a versatile platform for creating nanoparticle receptors to bind all kinds of molecules in water.[55-57] In this work, we have shown that the surface-cross-li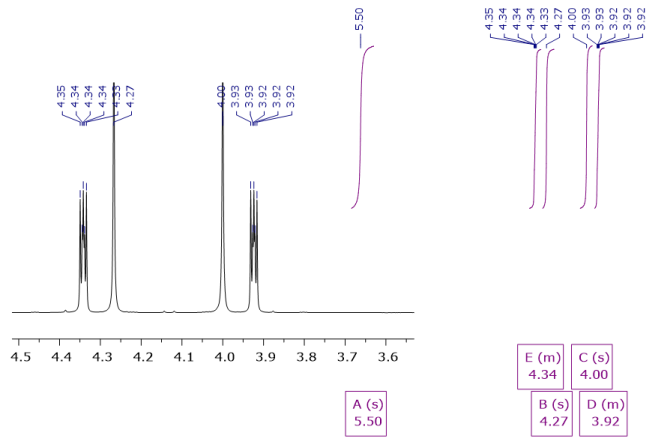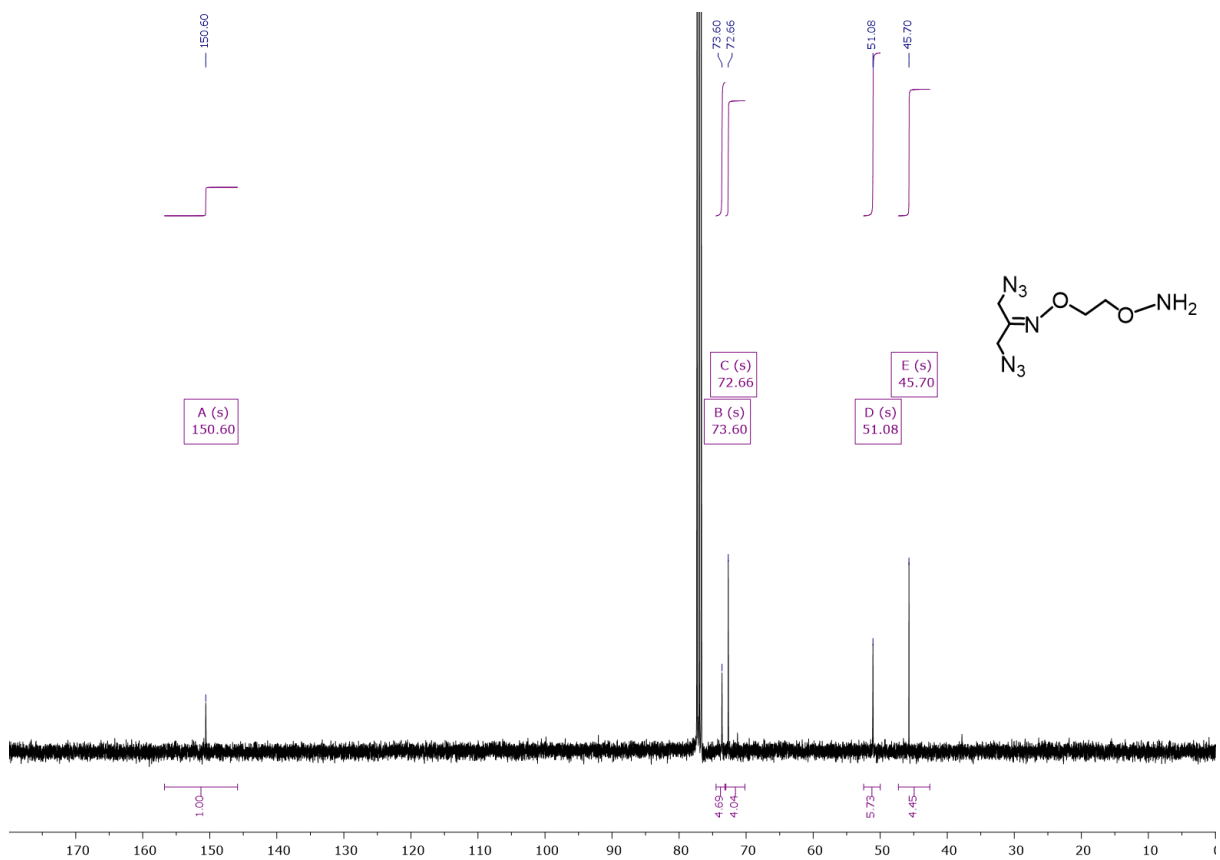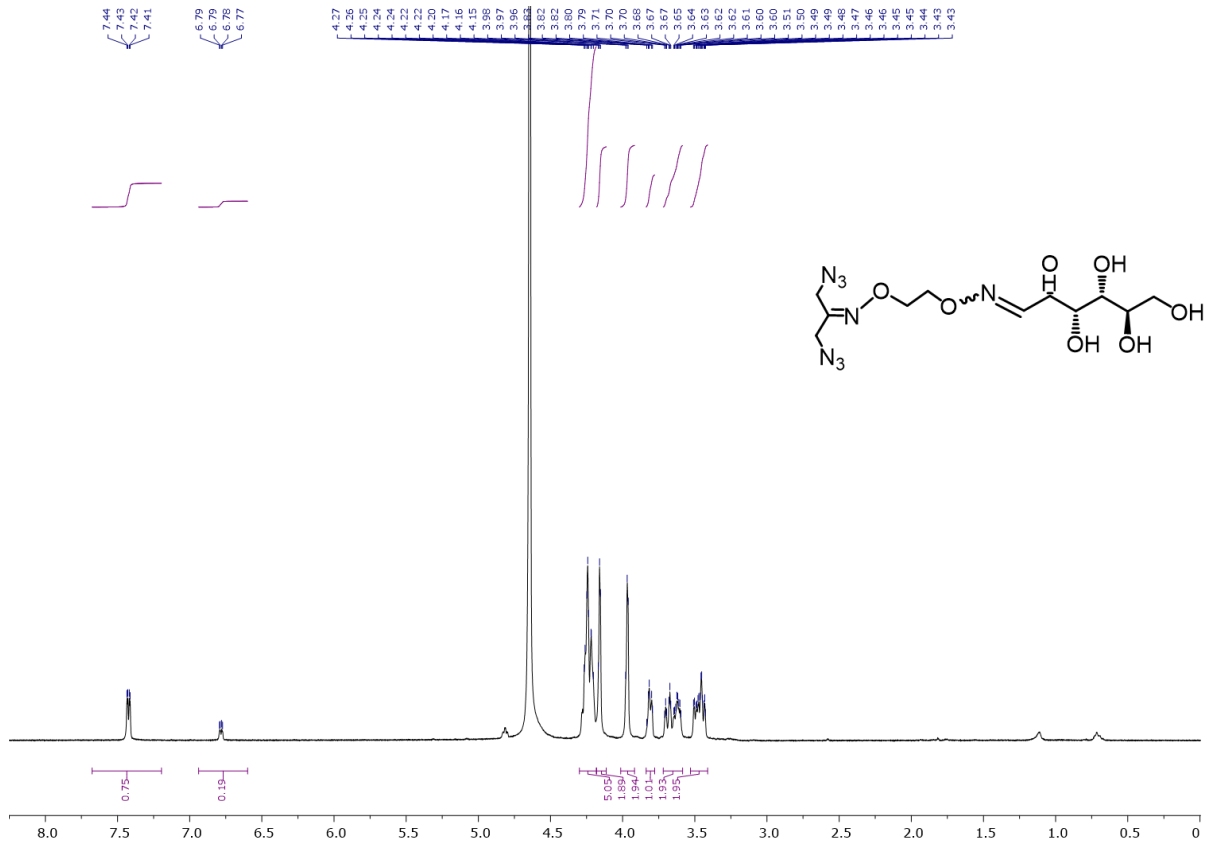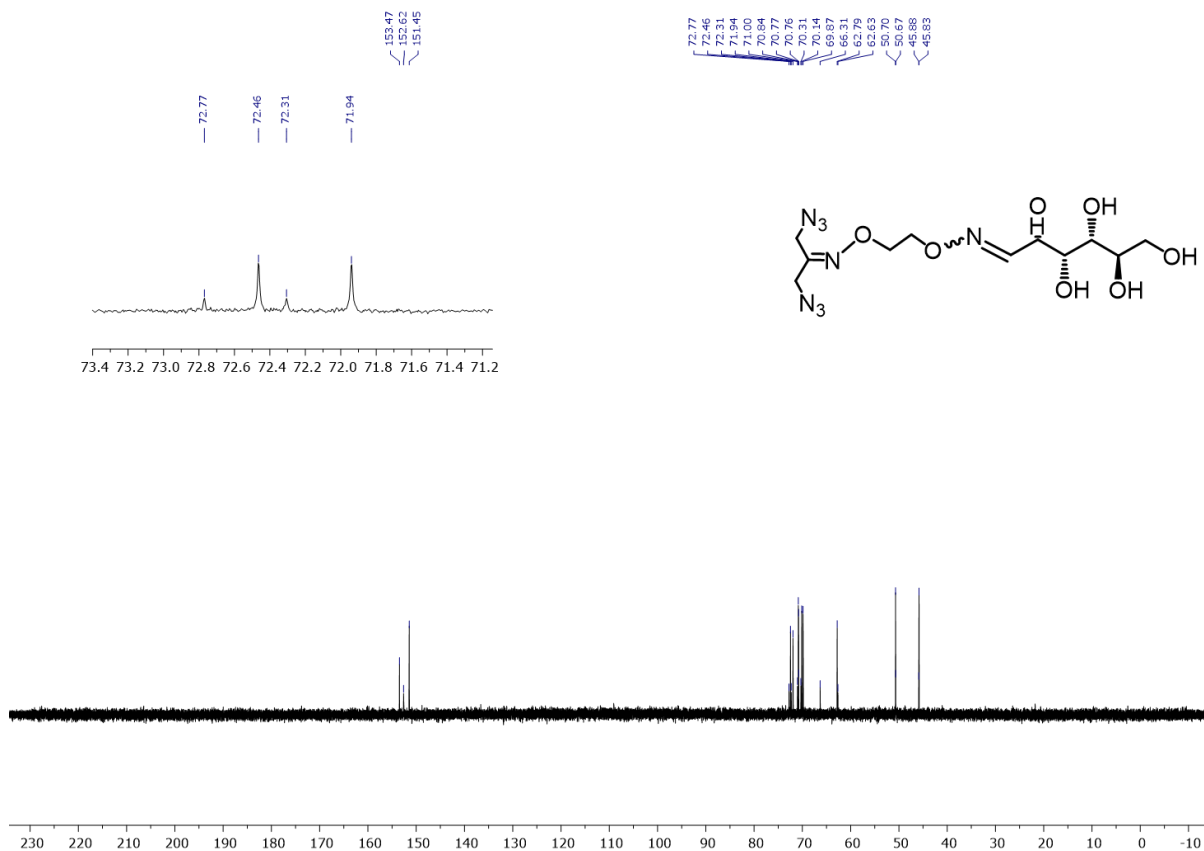nker could be tuned rationally to enhance the binding properties of MINPs. Shortening the tethers between the two azides by even one carbon clearly helped the binding, most likely by keeping the binding pockets in the open state prior to binding. Two-stage double surface-cross-linking was another useful strategy, enabled by the multifunctionality of compound **22**. The two-stage cross-linking could not only increase the surface-cross-linking density of the MINP but also expand the imprinted binding site into the polar region of the cross-linked micelle. It is important that these strategies can help any guests, ionic or nonionic, in terms of binding affinity and selectivity. Favorable hydrogen-bonding interactions could also be introduced through this strategy between the hydrophilic portion of the template and the MINP. Finally, good water-solubility is key to the performance of the surface-cross-linker. Although micelles have certain capacity to solubilize hydrophobic molecules in water, our formulation normally includes 1 equivalent of DVB to the cross-linkable surfactant. Since this is the highest amount of DVB that could be solubilized by surfactant **4** in the micelle,[55] it is good not to "burden" the micelle with any additional nonpolar solutes such as a poorly water-soluble surface-cross-linker.

REFERENCES

(1) Samuel H., G. *Chem. Rev.,* **1997**, 97, 12312.

(2) Jean-Marie, L. *Angew. Chem. Int. Ed. Engl.* **1990**, 29, 1304.

(3) Ji, X.; Li, J.; Chen, J.; Chi, X.; Zhu, K.; Yan, X.; Zhang, M.; Huang, F. *Macromolecules* **2012**, 45, 6457.

(4) Gassensmith, J. J.; Kim, J. Y.; Holcroft, J. M.; Farha, O. K.; Stoddart, J. F.; Hupp, J. T.; Jeong, N. C. *J. Am. Chem. Soc*. **2014**, 136, 8277.

(5) Kim, E.; Kim, D.; Jung, H.; Lee, J.; Paul, S.; Selvapalam, N.; Yang, Y.; Lim, N.; Park, C.; Kim, K. *Angew. Chem., Int. Ed.* **2010**, 49, 4405.

(6) Wulff, G.; Sarhan, A.; Zabrocki, K. *Tetrahedron Lett*. **1973**, 4329.

(7) Haupt, K.; Mosbach, K. *Chem. Rev.* **2000,** 100, 2495.

(8) Wulff, G. *Angew. Chem. Int. Ed. Engl.* **1995**, 34, 1812.

(9) Wulff, G. *Pure Appl. Chem.* **1982**, 54, 2093.

(10) Mosbach, K.; Haupt, K. *J. Mol. Recogn.* **1998**, 11, 62.

(11) Davankov, V. A.; Semechkin, A. V. *J. Chromatogr*. **1977**, 141, 313.

(12) Wulff, G.; Schauhoff, S. *J. Org. Chem*. **1991**, 56, 395.

(13) Awino, J. K.; Gunasekara, R. W.; Zhao, Y. *J. Am. Chem. Soc*. **2016**, 138, 9759.

(14) Wulff, G.; Minarik, M. *J. Liquid Chromatogr.* **1900**, 102, 706.

(15) Moradian, A.; Mosbach, K. *J. Mol. Recognit*. **1989**, 2, 167.

(16) Shea, K. J.; Thompson, E. A. *J. Org. Chem*. **1978**, 43, 4253.

(17) Whitcombe, M. J.; Rodriguez, M. E.; Vulfson, E. N. *Spec. Publ. R. Soc. Chem.* **1994**, 158, 565

(18) Wulff, G.; Heide, B.; Helfmeier, G. *J. Am. Chem. Soc*. **1986**, 108, 1089.

(19) Wulff, G.; Best, W.; Akelah, A. *React. Polym. Ion Exch. Sorb.* **1984**, 2, 167.

(20) Alexander, C.; Andersson, H. S.; Andersson, L. I.; Ansell, R. J.; Kirsch, N.; Nicholls, I. A.; O'Mahony, J.; Whitcombe, M. J. *J. Mol. Recognit*. **2006**, 19, 106.

(21) Kim, J. M.; Chong, B. O.; Ahn, K. D. *Anal. Lett*. **1998**, 31, 973.

(22) Dong, H.; Tong, A. J.; Li, L. D. *Spectrochim. Acta. A*. **2003**, 59, 279.

(23) Kempe, M. *Lett. Pept. Sci*. **2000**, 7, 27.

(24) Haginaka, J.; Sanbe, H. *Chem. Lett*. **1999**. 28, 757.

(25) Sellergren, B.; Shea, K. J. *J. Chromatogr.* **1993**, 654, 17.

(26) Kempe, M.; Fischer, L.; Mosbach, K. *J. Mol. Recognit*. **1993**, 6, 25.

(27) Piletsky, S. A.; Fedoryak, D. M.; Kukhar, V. P. *Chem. Abstr*. **1991**, 114, 165457q.

(28) Sellergren, B.; Ekberg, B.; Mosbach, K. *J. Chromatogr.* **1985**, 347, 1.

(29) Sarhan, A.; Wulff, G. *Makromol. Chem.* **1982**, 183, 1603.

(30) Wulff, G.; Schonfeld, R. *Adv. Mater*. **1998**, 10, 957.

(31) Fujii, Y.; Matsutani, K.; Kikuch, K. *J. Chem. Soc. Chem. Commun*. **1985**, 415.

(32) Fujii, Y.; Kikuchi, K.; Matsutani, K.; Ota, K.; Adachi, M.; Syoji, M.; Haneishi, I.; Kuwana, Y. *Chem. Lett*. **1984**, 1487.

(33) Hart, B. R.; Shea, K. J. *Macromolecules*. **2002**, 35, 6192.

(34) Kempe, M.; Glad, M.; Mosbach, K. *J. Mol. Recogn*. **1995**, 8, 35.

(35) Millar, J. R.; Smith, D. G.; Kressman, T. R. E. *J. Chem. Soc.* **1965**, 304.

(36) Wulff, G.; Vesper, W. *J. Chromatogr.* **1978**, 167, 171.

(37) Wulff, G.; Poll, H-G.; Minarik, M. *J. Liq. Chromatogr*. **1986**, 9, 385.

(38) Wulff, G.; Kemmerer, R.; Vietmeier, J.; Poll, H-G. *Nouv. J. Chem*. **1982**, 6, 681.

(39) Wulff, G.; Vietmeier, J.; Poll, H-G. *Makromol. Chem.* **1987**, 188, 731.

(40) Piletsky, S. A.; Piletskaya, K.; Piletskaya, E. V.; Yano, K.; Kugimiya, A.; Elgersma, A. V.; Levi, R.; U Kahlow.; Takeuchi, T.; Karube, I.; Panasyuk, T. I.; El'Skaya, A. V. *Anal. Lett.* **1996**, 29, 157.

(41) Gao, S. H.; Wang, W.; Wang, B. H. *Bioorg. Chem*. **2001**, 29, 308.

(42) Levi, R.; McNiven, S.; Piletsky, S. A.; Cheong, S. H.; Yano, K.; Karube, I. *Anal. Chem*. **1997**, 69, 2017.

(43) Marx-Tibbon, S.; Willner, I. *J. Chem. Soc., Chem. Commun*. **1994**, 1261.

(44) Mathew-Krotz, J.; Shea, K. J. *J. Am. Chem. Soc*. **1996**, 118, 8154.

(45) Mayes, A. G.; Andersson, L. I.; Mosbach, K. *Anal. Biochem*. **1984**, 222, 483.

(46) Ramstrom, O.; Nicholls, I. A.; Mosbach, K. *Tetrahedron. Asymmetry*. **1994**, 5, 649.

(47) Andersson, L. I.; Muller, R.; Mosbach, K. *Macromol. Rapid Commun*. **1996**, 17, 65.

(48) Ohkubo, K.; Funakoshi, Y.; Sagawa, T. *Polymer.* **1996**, 27,17, 3993.

(49) Liu, X.; Mosbach, K. Macromol. Rapid Commun. **1997**, 18, 609.

(50) Zhang, Y.; Deng, C.; Liu, S.; Wu, J.; Chen, Z.; Li, C.; Lu, W. *Angew. Chem. Int. Ed*. **2015**, 54, 5157.

(51) Shen, X.; Svensson Bonde, J.; Kamra, T.; Bulow, L.; Leo, J. C.; Linke, D.; Ye, L. *Angew. Chem. Int. Ed*. **2014**, 53, 10687.

(52) Hayden, O.; Lieberzeit, P. A.; Blaas, D.; Dickert, F. L. *Adv. Funct. Mater*. **2006**, 16, 1269.

(53) Pan, G.; Shinde, S.; Yeung, S. Y.; Jakstaite, M.; Li, Q.; Wingren, A. G.; Sellergren, B. *Angew. Chem. Int. Ed*. **2017**, 56, 15959.

(54) Golabia, M.; Kuralayb, F.; Jagera, E.; Beni, V.; Turner, A. *Biosens. Bioelectron*. **2017**, 93, 87.

(55) Awino, J. K.; Zhao, Y. *J. Am. Chem. Soc*. **2013**, 135, 34, 12552.

(56) Gunasekara, R. W.; Zhao, Y. *J. Am. Chem. Soc*. **2017**, 139, 829.

(57) Fa, S.; Zhao, Y. *Chem. Mater.* **2017**, 29, 9284.

(58) Whitcombe, M. J.; Rodriguez, M. E.; Villar, P.; Vulfson, E. N. *J. Am. Chem. Soc*. **1995**, 117, 7105.

(59) Andersson, L.; Ekberg, B.; Mosbach, K. *Tetrahedron Lett*. **1985**, 26, 3623.

(60) McKay, C. S.; Finn, M. G. Chemistry & Biology. 2014, 21, 9, 1075.

(61) Shankar, B. B.; Kirkup, M. P.; McCombie, S. W.; Ganguly, A. K. *Tetrahedron. Letters*. **1993**, 34, 45, 7171

(62) Oshovsky, G.V.; Reinhoudt, D.N.; Verboom, W.; Supramolecular chemistry in water. *Angew. Chem. Int. Ed.* **2007**, 46,2366-2393.